

Idaho National Engineering Laboratory

Operated by the U.S. Department of Energy

Semiscale Mod-2A Intermediate Break Test Series—Test Results Comparison

Timothy J. Boucher
Richard A. Dimenna

January 1983

Prepared for the

U.S. Nuclear Regulatory Commission

Under DOE Contract No. DE-AC07-76ID01570
B303150614 B30228
PDR NUREG
CR-3126 R PDR



Available from

GPO Sales Program
Division of Technical Information and Document Control
U.S. Nuclear Regulatory Commission
Washington, D.C. 20555

end

National Technical Information Service
Springfield, Virginia 22161

NOTICE

This report was prepared as an account of work sponsored by an agency of the United States Government. Neither the United States Government nor any agency thereof, nor any of their employees, makes any warranty, expressed or implied, or assumes any legal liability or responsibility for any third party's use, or the results of such use, of any information, apparatus, product or process disclosed in this report, or represents that its use by such third party would not infringe privately owned rights.

NUREG/CR-3126
EGG-2238
Distribution Category: R2

SEMISCALE MOD-2A INTERMEDIATE BREAK TEST SERIES – TEST RESULTS COMPARISON

Timothy J. Boucher
Richard A. Dimenna

Published January 1983

EG&G Idaho, Inc.
Idaho Falls, Idaho 83415

Prepared for the
U. S. Nuclear Regulatory Commission
Washington, D.C. 20555
Under DOE Contract No. DE-AC07-76IDO1570
FIN No. A6038

ABSTRACT

Results are presented from an analysis of Semiscale Mod-2A Intermediate Break Tests S-IB-1, -2, and -3. The tests were 100% (percentage of cold leg pipe flow area), 50%, and 21.7%, respectively, communicative cold leg break loss-of-coolant experiments. They were intended to provide reference data for evaluation and assessment of reactor safety code capabilities to predict integral blowdown, refill/reflood experiments for intermediate break sizes, and, particularly, to provide data to extend the code into the reflood regime. Comparisons of Semiscale intermediate break test results with those from large and small break tests provided characterization of the phenomena observed during the intermediate break tests. An additional objective of Test S-IB-3 was to provide reference data for comparison of Semiscale test results with results from LOFT Test L5-1 and LOBI Test B-R1M.

SUMMARY

The Semiscale experimental program conducted by EG&G Idaho, Inc., is part of the overall research and development program sponsored by the U.S. Nuclear Regulatory Commission (NRC) through the Department of Energy (DOE) to evaluate the behavior of pressurized water reactor (PWR) systems during hypothesized accident sequences. The primary objective of the Semiscale program is to obtain representative integral and separate-effects thermal-hydraulic response data to provide an experimental basis for analytical model development and assessment. This report presents results obtained from the Semiscale Mod-2A Intermediate Break Test Series. The Mod-2A system is a small-scale, nonnuclear experimental system in which nuclear heating is simulated by an electrically heated core. The system includes a vessel and two operating loops, both of which contain an active steam generator. The Semiscale intermediate break experiments were performed at typical PWR system pressures and temperatures.

Results from large and small break experiments performed in the Semiscale facility have previously been analyzed and characteristics of the different phenomena observed were identified. During large break experiments, the thermal-hydraulic response of the system is characterized by flow reversal at the core inlet, causing a flow split to occur in the core and leading to rapid voiding of the core. The inertially driven large flow rates cause rapid voiding of the loop pump suction and steam generator tubes, which in turn causes early decoupling of the primary and secondary systems. The high flow rate, low quality conditions in the core lead to a departure from nucleate boiling (DNB) on the surface of the heater rods while the rods have a high level of stored energy. This causes almost immediate, severe temperature excursions. In contrast, the thermal-hydraulic response of the system during small cold leg break experiments is characterized by a gravity driven draining of the system from upper elevations downward. After the horizontal sections of the loops have voided, pump suction and steam generator U-tube liquid forms a seal which restricts steam flow from the vessel. This causes a level depression in the vessel, which continues until the loop seals are cleared and the level in the vessel is able to recover. After vessel level recovery, there is a slow boiloff of liquid in the

core. The slow voiding of the pump suction and steam generator U-tubes allows the primary-to-secondary heat transfer to contribute to system energy removal. During the periods of vessel level depression, high quality, low flow conditions occur in the core, which can lead to dryout of the heater rods. This leads to minor temperature excursions which continue until the vessel level recovers after loop seal clearing. Additional dryouts of the heater rods can occur during the period of coolant boiloff, causing a second, minor temperature excursion prior to level recovery from emergency core cooling system injection.

Comparisons of the results of the intermediate break tests with large and small break test results provided a means to characterize the phenomena observed during each of the intermediate break tests. The hydraulic responses of the system observed during the 100^a and 50% break tests were found to be characterized by rapid voiding of the primary system due to large inertially driven flows, similar to the response observed during the large (200%) break test. The hydraulic response of the system during the 21.7% break test, however, was found to be characterized by gravity draining from upper elevations downward, leading to loop seal formation and vessel level depression. The vessel level was observed to recover after loop seal clearing, followed by a slow boiloff of core coolant. This was very similar to the hydraulic response observed for a small (10%) break test. The thermal response of the system during the 100% break test was characterized by the occurrence of a severe temperature excursion while the rods had a high level of stored energy, similar to the response observed during the large break test. In contrast, the thermal responses during the 50 and 21.7% break tests were characterized by a less severe temperature excursion while the rods were at decay heat levels. In the case of the 21.7% break test, two temperature excursions occurred; the first was caused by a vessel level depression, and the second was due to boiloff of core coolant. This was very similar to the thermal response observed during the small break test.

a. The 200, 100, 50, 21.7, and 10% break percentages correspond to full-scale equivalent break opening diameters of 38.9, 27.5, 19.4, 12.8, and 8.7 in., respectively.

Comparisons between Loss-of-Fluid Test (LOFT) facility and Semiscale intermediate break test results show good agreement, except during portions of the transients in which facility configuration differences preclude similar system hydraulic responses.

Results of comparisons between Loop Blow-down Investigation (LOBI) facility (Ispra, Italy) and Semiscale intermediate break data indicate that the results from the counterpart test performed in the Semiscale facility repeated the results from the LOBI B-RIM test quite well. The hydraulic responses during both tests were characterized by gravity draining, loop seal formation leading to vessel level depression, and boiloff of core coolant following vessel level recovery. The extent of the vessel level depressions were found to differ due to pump suction elevation differences. Additionally, sensitivity calculations indicate that late isolation of the intact loop steam generator steam line during Semiscale Test S-IB-3 caused a delayed clearing of the intact loop seal. Thus, slight differences noted in the hydraulic responses

were due to facility configuration and test conduct differences. The thermal responses during the tests also showed some discrepancies. No temperature excursion occurred during Test B-RIM, whereas two temperature excursions occurred during Test S-IB-3. Sensitivity calculations indicate that the differences in heater rod designs and axial power profiles had very little effect on the test results. The differences in the thermal responses were determined to be due to the large volume of the LOBI downcomer gap (50 mm) and the deeper positioning and longer heated length of the LOBI core.

In summary, the "dividing line" between large and small breaks appears, on the basis of the general phenomena that should be emphasized for modeling purposes, to be somewhere between 50 and 21.7%. Furthermore, comparisons of Semiscale results with LOFT and LOBI results indicate that the basic scaling rationale common to these facilities preserves the thermal-hydraulic phenomena across scale sizes ranging from 1/1700 to 1/60.

ACKNOWLEDGMENTS

The authors gratefully acknowledge the technical contributions of G. W. Johnsen, T. K. Larson, J. S. Martinell, and J. L. Perryman in reviewing this report. We also acknowledge the contributions from all those who worked on the quick look reports for the experiment series and T. K. Larson and D. J. Shimeck for providing insight to the general phenomena which characterize large and small breaks.

CONTENTS

ABSTRACT	ii
SUMMARY	iii
ACKNOWLEDGMENTS	v
1. INTRODUCTION	1
2. SEMISCALE SYSTEM CONFIGURATION AND TEST CONDUCT	2
2.1 System Configuration	2
2.2 Test Conduct	4
3. TEST RESULTS COMPARISON	7
3.1 Characteristics of Large and Small Breaks	7
3.1.1 Hydraulic Response During Large and Small Breaks	7
3.1.2 Thermal Response During Large and Small Breaks	7
3.2 Comparison of Semiscale Large, Intermediate, and Small Break Data	8
3.2.1 Description of Semiscale Tests Used for Comparisons	8
3.2.2 Hydraulic Response During Large, Intermediate, and Small Breaks	8
3.2.3 Thermal Response During Large, Intermediate, and Small Breaks	17
3.3 Comparison of Semiscale and LOFT Intermediate Break Data	19
3.3.1 Comparison of Thermal-Hydraulic Responses During Semiscale Test S-IB-3 and LOFT Test L5-1	20
3.4 Comparison of Semiscale and LOBI Intermediate Break Data	25
3.4.1 Comparison of Thermal-Hydraulic Responses During Semiscale Test S-IB-3 and LOBI Test B-R1M	26
3.4.2 Effects of Facility Configuration Differences	33
3.4.3 Effects of Differences in Test Conduct	36
4. CONCLUSIONS	38
5. REFERENCES	39
APPENDIX A—RELAP5 SENSITIVITY STUDIES	41

SEMISCALE MOD-2A INTERMEDIATE BREAK TEST SERIES—TEST RESULTS COMPARISON

1. INTRODUCTION

Testing performed in the Semiscale Mod-2A facility is part of the water reactor safety research effort directed toward assessing and improving the analytical capability of computer codes used to predict the behavior of pressurized water reactors (PWRs) during postulated accident scenarios. For this purpose, the Mod-2A system was designed as a small-scale model of the primary system of a four-loop PWR nuclear generating plant. The system incorporates the major components of a PWR, including steam generators, vessel, pumps, pressurizer, and loop piping. The intact loop is scaled to simulate the three intact loops in a PWR, whereas the broken loop simulates the single loop in which a break is postulated to occur in a PWR. Geometric similarity has been maintained between a PWR and the Mod-2A system, most notably in the design of a 25-rod, full-length (3.66 m), electrically heated core; full-length upper head and upper plenum; component layout; and relative elevations of various components. Equipment in the upper head of the Mod-2A vessel has been designed to simulate the fluid flow paths found in a PWR having the inverted top hat upper head internals package.^a The scaling philosophy followed in the design of the Mod-2A system (modified volume scaling) preserves most of the important first-order effects thought to be important during loss-of-coolant transients.²

This report presents an analysis of data from Semiscale Mod-2A Intermediate Break Tests S-IB-1, -2, and -3. The tests were 100, 50, and 21.7%, respectively, communicative cold leg break loss-of-coolant experiments. The primary objective of Tests S-IB-1 and -2, and a secondary objective of

Test S-IB-3, was to provide reference data for evaluation and assessment of reactor safety code capabilities to predict integral blowdown, refill/reflood experiments for intermediate break sizes. The primary objective of Test S-IB-3 was to provide reference data for comparison of Semiscale test results with results from the Loop Blowdown Investigation (LOBI) facility (Ispra, Italy) B-R1M³ test. Another important objective of all three Semiscale tests was to expand the break spectrum data base to cover the 10 to 200% range in order to determine if other phenomena are important to core cooling and to evaluate the Mod-2A system response to breaks in this range.

Specific topics included in this report are: characterization of phenomena observed during large and small breaks; comparison of Semiscale large, intermediate, and small break data; brief comparison of Semiscale and Loss-of-Fluid Test (LOFT) facility (EG&G Idaho) intermediate break data; and, finally, a comparison of Semiscale and LOBI intermediate break data, including the effects of system configuration and test conduct differences on test results. Comparisons of the results of the Semiscale and LOBI tests are important for several reasons. First, comparisons of the test data provide a means of assessing the similarity of results obtained during nearly identical tests performed in the two facilities. Similarity in results over several scale sizes verifies the scaling philosophy applied to the facilities and lends credence to the usefulness of the results obtained by these facilities for code assessment purposes. Secondly, comparisons of the test results provide a means of investigating the characteristics peculiar to each of the facilities. Examination of the behavioral differences between the systems highlights the significant roles that certain configurational aspects have in influencing the test results.

a. This is a recent modification to the Semiscale Mod-2A reactor vessel upper head. The modification is described in Reference 1.

2. SEMISCALE SYSTEM CONFIGURATION AND TEST CONDUCT

2.1 System Configuration

The intermediate break experiments were performed in the Semiscale Mod-2A test facility, which is a 17.2-MPa, 616-K stainless-steel-type system scaled to model the primary system of a four-loop PWR nuclear generating plant (scaling factor 1/1705). The system incorporates the major components of a PWR, including steam generators, vessel, downcomer, pumps, pressurizer, and loop piping as shown in Figure 1. The loop piping consists of an intact loop and a broken loop, the former representing three of the four loops in a PWR, the latter simulating the single loop in which a break is postulated to occur in a PWR. The pressurizer is connected to the intact loop hot leg, and the pressure suppression header and tank are connected via the rupture disk assembly to the broken loop cold leg. Emergency core coolant from an accumulator and high or low pressure injection system pumps is routed to the loop cold legs. An open loop secondary coolant system is used.

In Semiscale, the annular downcomer of a PWR vessel is replaced with an external pipe to permit extensive instrumenting of both the core and downcomer regions. Most of the fluid system components are full height, including the core, which consists of a 5 x 5 array of electrically heated, 3.66-m-long, 1.072-cm-outside-diameter rods which simulate the fuel rods in a 15 x 15 type PWR core. The number of turns per inch of the electrical heating coil is varied along the rod length to give the staircase approximation of a cosine axial heat flux shape. Equal power was applied to the 23 heated rods; two of the rods were unpowered.

The upper head, upper plenum, and core flow bypass arrangement in the Semiscale reactor vessel was modified in November 1981 to better simulate a Westinghouse inverted top hat, upper head internals package design.¹

All of the intermediate break tests involved a break at the horizontal midplane of the cold leg pipe, between the broken loop pump and downcomer inlet, and at a position relative to that pipe simulating a break in its wall. This was accomplished by utilizing a communicative break

assembly, with break orifice or break nozzle and rupture disk assembly connected to the pressure suppression (containment simulation) system. For Tests S-IB-1 and -2, the orifices were sized to simulate a break area of 100 and 50%, respectively, of the cold leg in a PWR. For Test S-IB-3, the converging diverging nozzle was sized to preserve the ratio of break area to system volume for the LOBI B-R1M test. This resulted in a simulated break area of 21.7% of the cold leg in a PWR. The entrances of both orifices and the nozzle were elliptical in shape.

For all of the intermediate break tests, the accumulator and high or low pressure injection system pumps were routed to the intact loop only. For Test S-IB-3, only the accumulator and low pressure injection system were utilized for emergency core coolant.

The intact loop steam generator is a tube and shell design. Primary fluid flows through vertical, inverted-U-shaped tubes and secondary coolant passes through the shell side. The intact loop steam generator has two short, two medium, and two long tubes representative of the range of bend elevations in a PWR steam generator. The same tube stock (2.22-cm OD x 0.124-cm wall) and tube spacing (3.175-cm triangular pitch) used for PWR U-tubes were used in the steam generator. Since the heat transfer area was specified based on the ratio of PWR to Semiscale core power, the number of tubes was thereby fixed by the specified tube diameter and length. Fillers are installed in the shell side to provide a more properly scaled secondary fluid volume. Elevations of steam generator nozzles, plenums, and tubes are similar to those of a PWR; however, the steam dome is shorter than that of a PWR. The broken loop steam generator is of similar design to the intact loop steam generator, except for the number of primary tubes. Since the broken loop simulates only one loop of a four-loop PWR, the broken loop steam generator has only a long tube and a short tube, both of which are identical to the corresponding intact loop tubes. Further details of the various components of the Mod-2A system can be found in Reference 1, and details of the Mod-2A system, as configured for the intermediate break test series, can be found in References 4 through 8.

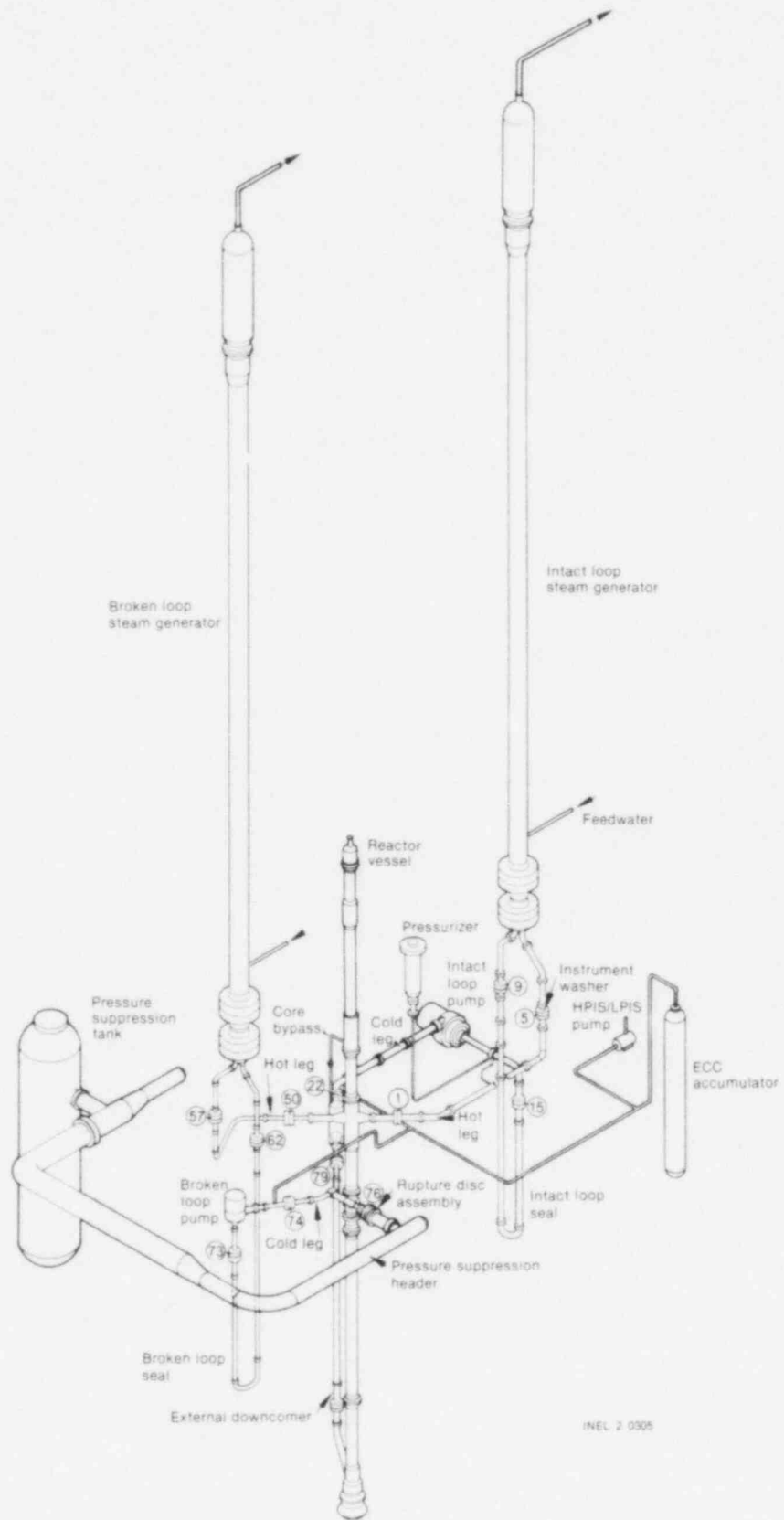


Figure 1. Semiscale Mod-2A system for Intermediate Break Test Series.

Conditions in the system were monitored by an extensive network of metal and fluid thermocouples and differential pressure transducers. In the steam generator, a long and short tube are extensively instrumented with both primary- and secondary-side fluid thermocouples and several primary-side differential pressure transducers. Average fluid density is measured in the loops and vessel with X-ray and gamma densitometers, volumetric flow is measured with turbine meters, and momentum flux is measured with drag screens. In addition, an optical probe was used to view the break nozzle assembly. Further details of the measurement system and control system configurations for the intermediate break tests can be found in References 4 through 8.

2.2 Test Conduct

Three transient experiments were performed in the Semiscale Mod-2A facility. These experiments simulated intermediate break loss-of-coolant

accidents (LOCAs) involving break areas representative of 100, 50, and 21.7% of the area of the cold leg in a PWR. Table 1 summarizes the specified initial conditions for each of the tests and a comparison of the specified and actual initial conditions can be found in References 6 through 8.

A brief narrative describing the control of events during the tests follows. The exact timing of the occurrence of the controlled events can be found in Table 2. Immediately after rupture of the pressure boundary, the core power and pump speeds began following controlled transients. Shortly after the pressurizer pressure reached 12.6 MPa, the intact and broken loop steam generator steam valves were closed.^a This was followed by closure of the intact and broken loop steam generator feedwater valves. Approximately

a. During the 21.7% break test (S-IB-3), the intact loop steam generator steam valve was not closed until the primary system pressure reached 1 MPa.

Table 1. Specified initial conditions for the intermediate break tests

	S-IB-1 and S-IB-2	S-IB-3
Primary Coolant System		
Intact/broken loop flow rate	3:1	3:1
Pressurizer pressure (MPa)	15.5 ± 0.2	15.5 ± 0.2
Core temperature rise (K)	37 ± 2	33 ± 2
Cold leg fluid temperature (K)	557 ± 2	563 ± 2
Core flow rate (kg/s)	9 to 10	7 to 8
Pressurizer liquid mass (kg)	10.4 ± 0.1	8.2 ± 0.1
Total core electrical power (MW)	1.95 ± 0.05	1.44 ± 0.05
Secondary Coolant System		
Steam generator steam dome pressures (MPa)	5.8 ± 0.2	5.4 ± 0.2
Steam generator feedwater temperatures (K)	495 ± 2	483 ± 2
Coolant Injection System		
Intact loop accumulator		
Pressure (MPa)	4.24 ± 0.1	2.7 ± 0.1
Water volume (m ³)	0.048 ± 0.001	0.067 ± 0.001
Nitrogen volume (m ³)	0.025 ± 0.001	0.015 ± 0.001
Water temperature (K)	300 ± 10	305 ± 10

Table 2. Chronology of events for the intermediate break tests

Event	Time (s)		
	S-1B-1	S-1B-2	S-1B-3
Rupture initiated; core power, pump speed transients initiated	0	0	0
Upper plenum fluid saturates	<1	<1	1.5
Temperature excursion begins	1	29	50
Intact loop steam generator steam valve closed	8	8	240
Broken loop steam generator steam valve closed	8	8	5
Intact loop steam generator feedwater valve closed	25	15	30
Broken loop steam generator feedwater valve closed	25	15	2.5
HPIS flow starts	30	30	NA ^a
Accumulator flow starts	27	50	163
Power to broken loop pump tripped	50	100	240
Blowdown ends	55	103	240
LPIS flow starts	55	118	240
Accumulator empties of liquid	58	105	NA ^b
Lower plenum refilled; reflood starts	140	130	190
Core quenched	NA ^c	705	350
Data acquisition system shut down	487	1000	531

a. No HPIS flow was used during Test S-1B-3.

b. The accumulator did not empty during Test S-1B-3.

c. Not available—the core did not quench before the end of data acquisition time was reached.

25 to 30 s after the pressurizer pressure reached 12.6 MPa, high pressure injection system (HPIS) flow was initiated.^a Upon reaching a primary system pressure of 1 MPa, the power to the broken loop pump was tripped and LPIS flow was initiated shortly thereafter. The tests were terminated upon reaching the end of available data acquisition space.

Several of the events that occurred during the tests are described next. The depressurization of the primary system caused the vessel upper plenum fluid to reach saturation conditions within 1 to 2 s after rupture of the pressure boundary. As the vessel coolant was displaced from the core, the heater rod temperatures began to increase. The depressurization of the primary system continued

a. HPIS flow was not used during the 21.7% break test (S-1B-3) in order to simulate the lack of HPIS flow during the LOBI B-R1M test.

and the accumulator actuation pressure was reached, initiating accumulator injection. When the system pressure reached 1 MPa, the blowdown was essentially over and the accumulator emptied of liquid shortly thereafter.^b The flow of LPIS liquid had started by this time, the refilling of the vessel lower plenum was completed,^c and reflooding of the core was initiated. The reflooding of the vessel led to the eventual quench of the core.

b. A lower pressure setpoint and a larger volume of water was used in the accumulator during Test S-1B-3 to simulate the LOBI B-R1M test conditions. This allowed accumulator injection to continue through the end of the test.

c. During the 21.7% break test, the vessel lower plenum remained full throughout the transient. This allowed core reflooding to be initiated before the end of the blowdown.

3. TEST RESULTS COMPARISON

Results from large and small break experiments performed in the Semiscale facility have previously been analyzed, and characteristics of the different phenomena observed were identified. Comparisons of the intermediate break test results with those from large and small break tests provide a means to characterize the phenomena observed during each of the intermediate break tests. In addition, comparison of Semiscale test results with those obtained from other scaled facilities (the Loss-of-Fluid Test facility and the Loop Blowdown Investigation facility) aids in evaluating the validity of the scaling philosophy applied to the facility designs, as well as lending credence to the usefulness of the test results for computer code assessment purposes.

This section first presents a general characterization of the phenomena observed during large and small break tests in Semiscale, followed by a comparison of Semiscale large, intermediate, and small break data. The data from intermediate break tests in Semiscale and the Loss-of-Fluid Test facility are compared, as are the data from similar tests in the Loop Blowdown Investigation facility and Semiscale. This latter comparison includes an assessment of the effects of system configuration and test conduct differences on the test results.

3.1 Characteristics of Large and Small Breaks

Analysis of the results of large⁹ and small¹⁰ break tests performed in the Semiscale facility has enabled a determination of some of the important phenomena during such test. The following sections present a characterization of the different phenomena observed during large and small breaks.

3.1.1 Hydraulic Response During Large and Small Breaks. The hydraulic response observed during large break loss-of-coolant accident (LOCA) experiments in the Semiscale facility can be characterized in the following manner. After rupture of the pressure boundary, the flow at the inlet to the core reverses while the positive flow at the core outlet is maintained by the inertia of the fluid and by the break flow through the hot leg to the pump side of the break. This causes a flow split to occur in the core, which leads to rapid

voiding of the core. Because this is an inertially driven phenomenon, the resistance distribution in the system can affect the flow split in the core. The effect of the pumps on the hydraulic response is minimal due to the rapid degradation of the Semiscale pump heads with increasing void fraction. As the system depressurizes, the actuation pressure of the emergency core coolant accumulator is reached and accumulator injection is initiated. Following a period of flow bypass, the accumulator liquid is able to penetrate the downcomer and rapidly refill the lower plenum of the vessel, thus initiating reflooding of the core, which is continued by the low pressure injection system.

The hydraulic response observed during small, cold leg break LOCA experiments^a in the Semiscale facility is significantly different. Following rupture of the pressure boundary, the system voids from the upper elevations downward due to the hydrostatic head of the fluid in the system. After the horizontal sections of the loops void, the pump suction contains liquid which forms a seal and restricts the flow of steam from the vessel to the break. This causes the pressure to increase in the vessel relative to the downcomer, thus depressing the liquid level in the vessel. This level depression in the vessel continues until the loop seals clear and allow the system pressures to equilibrate and the level in the vessel to recover. After the vessel level recovers, there is a slow boiloff of liquid in the core. Because system voiding is slow, the pumps can affect the flows in the loops and the core. The decreasing system pressure serves to actuate the ECC accumulator, thus initiating injection of accumulator fluid. Following a brief period of "hold-up," the accumulator liquid penetrates the downcomer and initiates reflooding of the core, which is later augmented by the LPIS.

3.1.2 Thermal Response During Large and Small Breaks. Immediately following a large break, the high flow rate, low quality conditions

a. Small, cold leg break LOCA experiments have been performed in the Semiscale facility for break sizes ranging from 0.4 to 10%.

in the core lead to a departure from nucleate boiling (DNB) on the surface of the heater rods. At the time of DNB, the heater rods are still at stored energy levels and prompt fission power is still ongoing, which results in severe temperature excursions. Elevated temperatures generally continue to exist in the core until the vessel has reflooded to a level sufficient to allow low quality steam and water droplets to reach and rewet the surface of the heater rods. Due to the rapid voiding of the primary side of the system, the primary-to-secondary heat transfer is minimal and the steam generators have very little effect on the transient.

During a small break, the system voids from the upper elevations downward and the level is depressed in the vessel due to the formation of liquid seals in the pump suction. High quality, low flow conditions occur in the core which can lead to dryout of the heater rod surfaces. At the time of these dryouts, the heater rod power is at decay heat levels, resulting in less severe temperature excursions. The slightly elevated temperatures generally continue to exist in the core until the level in the vessel recovers, due to loop seal clearing, and low quality steam and water droplets reach and rewet the surface of the heater rods. After the vessel level recovers, a slow boiloff of liquid in the core can lead to additional dryouts of the heater rod surfaces. The temperature excursions that occur from this second dryout continue until the vessel is reflooded and the rods are rewet by the low quality steam and water droplets. The slow depressurization and slow voiding of the primary side of the system causes the primary-to-secondary heat transfer to be a major contributor to the removal of energy from the system. The steam generators, therefore, can have a substantial effect on the removal of energy from the core during a small break accident.

3.2 Comparison of Semiscale Large, Intermediate, and Small Break Data

The tests performed during the Intermediate Break Test Series were the first such LOCA experiments performed in the Semiscale facility. Thus, little was known about the general phenomena that are important during intermediate breaks in Semiscale. This section presents a description of the large and small break tests used for comparison with the intermediate break

tests, followed by discussions of the results from comparisons of the hydraulic and thermal responses during the three types of tests.

3.2.1 Description of Semiscale Tests Used for Comparisons. For the purposes of these comparisons, the tests chosen to represent the large and small break Semiscale system responses were selected for the typicality of their results to other such tests in Semiscale. Test S-07-8⁹ simulated a 200% noncommunicative break in the cold leg of a PWR between the downcomer inlet and pump. The test was performed in the Semiscale Mod-3 facility and utilized vessel lower plenum ECC injection. Test S-UT-1¹⁰ simulated a 10% communicative break in the cold leg of a PWR between the downcomer inlet and pump. The test was performed in the Semiscale Mod-2A facility. The three intermediate break tests simulated 100% (S-IB-1), 50% (S-IB-2), and 21.7% (S-IB-3) communicative breaks in the cold leg of a PWR between the downcomer inlet and pump, and were also performed in the Semiscale Mod-2A facility. To satisfy conservative assumptions, cold leg ECC injection into the intact loop only was utilized during the three intermediate break tests and Test S-UT-1. No high pressure injection system flow was used during Test S-IB-3 because the Loop Blowdown Investigation facility had no HPIS capabilities for the B-RIM test and Test S-IB-3 was a counterpart test. Although several minor differences in system configuration and test conduct exist between the five tests, these are not believed to have had a significant effect on the comparison results.

3.2.2 Hydraulic Response During Large, Intermediate, and Small Breaks. The hydraulic response of the system after rupture of the pressure boundary was very similar during the 200, 100, and 50% break tests. As shown in Figure 2, the break mass flow rates^a during the three tests showed quite similar trends. The flows were characterized by a large peak, followed by a rapid decrease as the homogeneous flow conditions at the break changed quickly from saturated liquid to vapor. The hydraulic response of the 21.7% break test was very similar to that of the 10% break test. Figure 3 shows the break mass flow rates^{a,b} during the two tests and indicates the

a. The break mass flow rates were calculated using the broken loop cold leg mass flows on each side of the break. Thus, slight differences in the initial condition measurements produced the unrealistic values prior to break initiation.

b. The longer timebase of the 10% break data causes the slight offset of the initiation of break flow from $t = 0$.

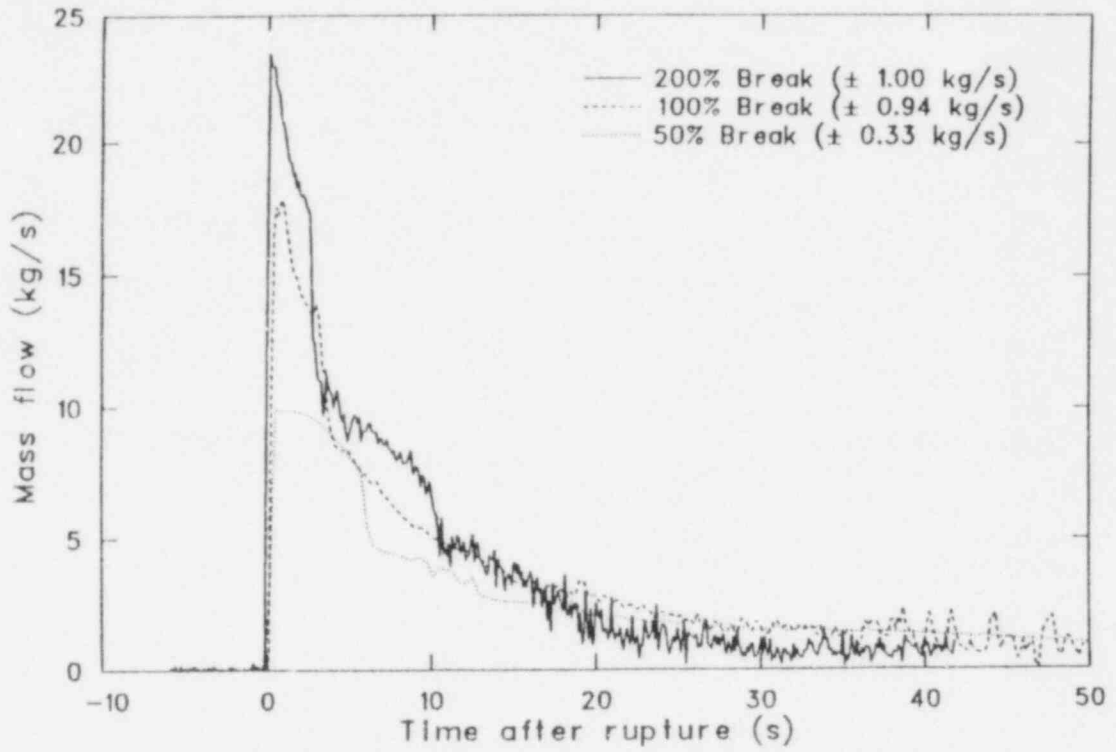


Figure 2. Comparison of break mass flow rates during the 200, 100, and 50% break tests.

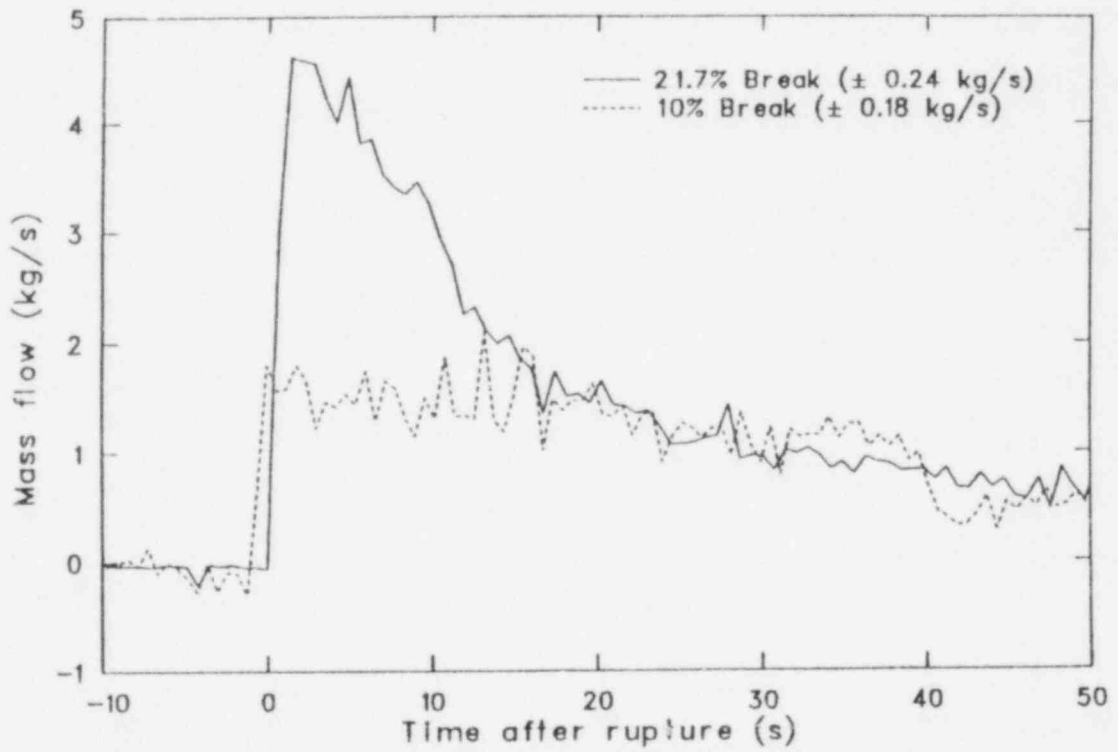


Figure 3. Comparison of break mass flow rates during the 21.7 and 10% break tests.

similar trends observed. The flows were characterized by a period of sustained flow, with a gradual decrease as the stratified flow conditions at the break caused gradual transition from sub-cooled liquid to saturated liquid and vapor, followed by vapor flow.

The relatively large, inertially dominated mass flow rates observed during the 200, 100, and 50% break tests led to a rapid depletion of vessel and downcomer coolant inventory during all three tests, as shown in Figures 4 through 6. The vessel was essentially devoid of coolant by about 20 s during the 200 and 100% break tests, and by about 40 s during the 50% break test. The relatively large mass flow rates during the three tests also caused the liquid to be cleared out of the loop pump suction early in the transients. The rapid rise of the vessel and downcomer levels observed at about 21 s in Figure 4 is due to the fact that the emergency core coolant was injected directly into the vessel lower plenum during the 200% break test. This prevented ECC accumulator liquid from bypassing the downcomer to the break, which occurs during large break tests utilizing cold leg injection. Thus, the accumulator liquid entered the vessel almost immediately after the initiation of injection, refilled the vessel lower

plenum, and initiated reflooding of the core. The core reflooding was continued by scaled, LPIS flow. Intact loop cold leg ECC injection was used during the 100 and 50% break tests.

Due to the single-pipe design of the Semiscale external downcomer, limited countercurrent flow occurs in the downcomer. Thus, an atypically large amount of accumulator liquid was bypassed from the intact loop cold leg to the break during the blowdown of the 100 and 50% break experiments. A comparison of Figures 5 and 6 with Figure 4 shows that the level increase due to accumulator liquid entering the downcomer and vessel was much more pronounced during the 200% break test than during the 100 and 50% break tests. The amount of accumulator liquid penetration during the 100% break test was also degraded due to a smaller liquid volume in the accumulator than the specified scaled volume. Hence, the refilling of the vessel lower plenum was completed and the reflooding of the core was driven by a low pressure injection system flow, which was lower than the specified scaled, degraded LPIS flow. This low LPIS flow caused the core level to be only 50 cm above the bottom of the heated length at the end of data acquisition time. The accumulator liquid penetration during

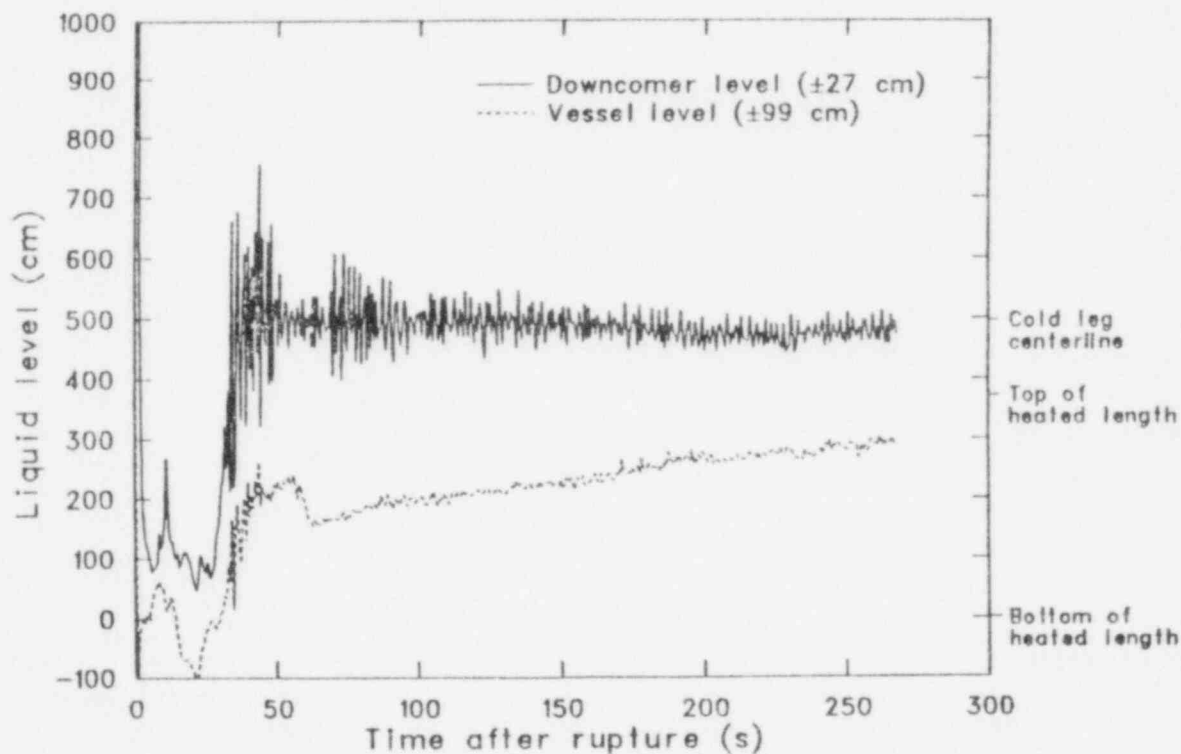


Figure 4. Vessel and downcomer collapsed liquid levels during the 200% break test (S-07-8).

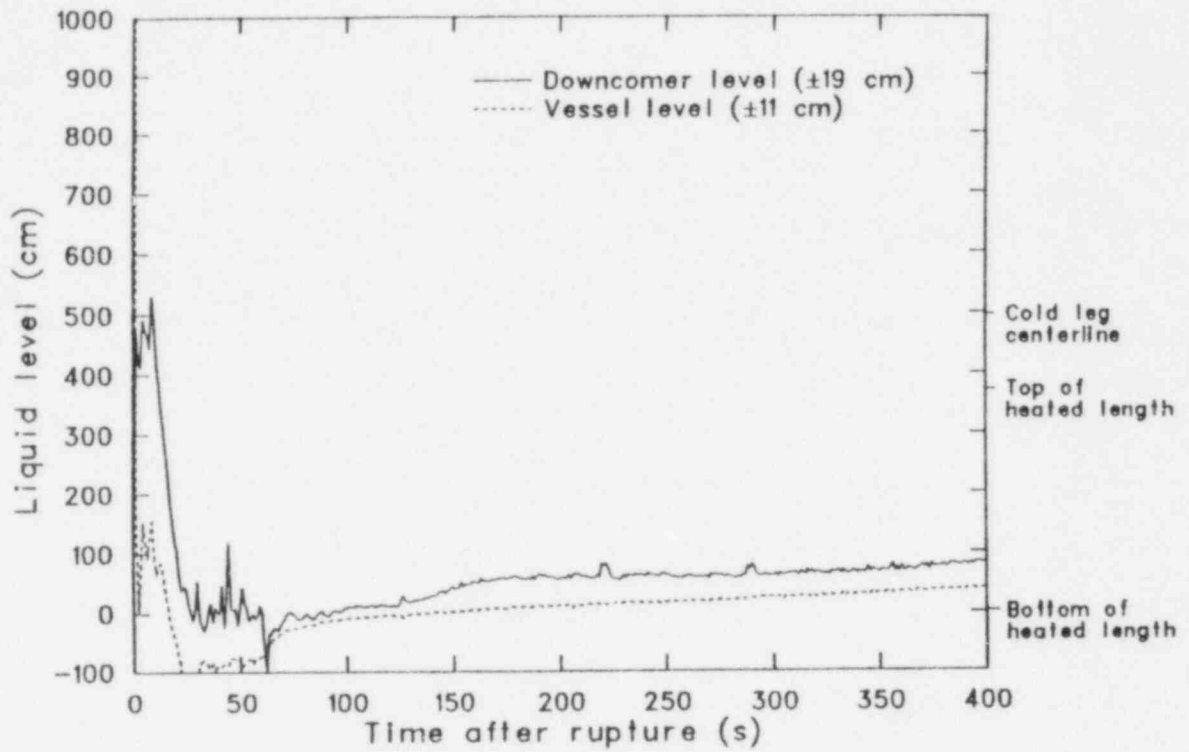


Figure 5. Vessel and downcomer collapsed liquid levels during the 100% break test (S-IB-1).

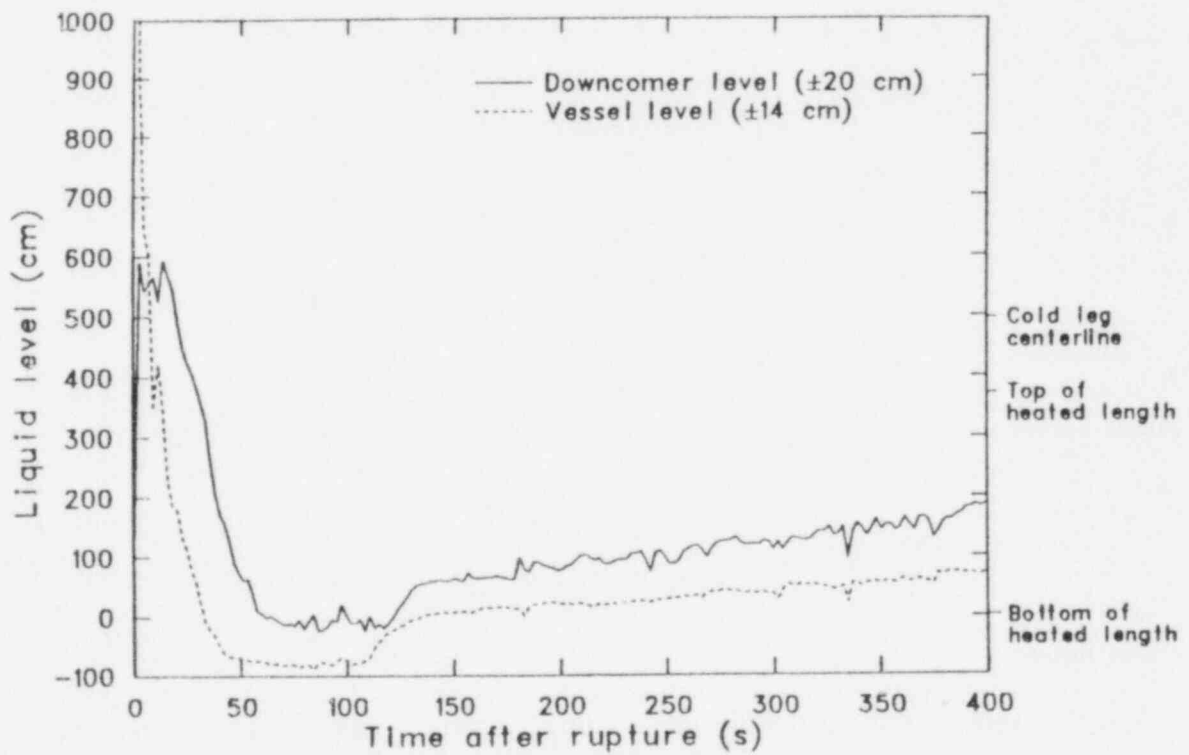


Figure 6. Vessel and downcomer collapsed liquid levels during the 50% break test (S-IB-2).

the 50% break test was sufficient to refill the vessel lower plenum; however, the reflooding of the vessel core was driven only by the scaled, degraded LPIS flow.

The relatively small, gravity-driven mass flow rates observed during the 21.7 and 10% break tests were not sufficient to cause rapid depletion of the vessel coolant inventory, nor were they sufficient to clear liquid out of the loop pump suction early in the transients. As shown in Figures 7 and 8, the minimum levels in the vessel during both tests occurred during a period of manometric imbalance between the vessel and downcomer. This manometric imbalance was due to a buildup of pressure in the vessel caused by liquid in the pump suction and steam generator U-tubes forming a seal and impeding steam flow through the loops. Figure 9 shows that the broken loop pump suction upflow leg cleared between 27 and 34 s, whereas the intact loop pump suction upflow leg was gradually swept clear between 89 and 150 to 160 s during the 21.7% break test.

The effect of the broken loop pump suction clearing is shown in Figure 7 as a stall in the vessel level depression, at approximately the elevation of the pump suction, between 34 and 40 s. However,

as shown in Figure 10, liquid was being held up in the intact loop steam generator tubes until 150 to 160 s. The U-tube liquid gravity head, combined with that of the intact loop pump suction, caused the vessel level to continue to depress after the broken loop pump suction cleared. The vessel level depression continued until sufficient pressure was built up in the vessel and intact loop hot leg to achieve the necessary pressure differential between the hot and cold legs to clear the intact loop steam generator U-tubes and pump suction. As shown in Figure 7, the manometric imbalance between the vessel and downcomer decreased as the intact loop pump suction and steam generator U-tubes cleared, and the vessel level recovered between 89 and 120 to 130 s. Slow boiloff of core coolant caused the vessel level to decrease between 130 and 190 s. At 190 s, ECC accumulator liquid penetrated the downcomer and initiated reflooding of the core.

Figure 11 indicates that the broken loop pump suction upflow leg was gradually swept clear between 20 and 140 to 150 s during the 10% break test, whereas the intact loop pump suction upflow leg swept out gradually between 90 and 150 to 160 s, after partially clearing at about 72 s. The effect of the partial clearing of the intact loop

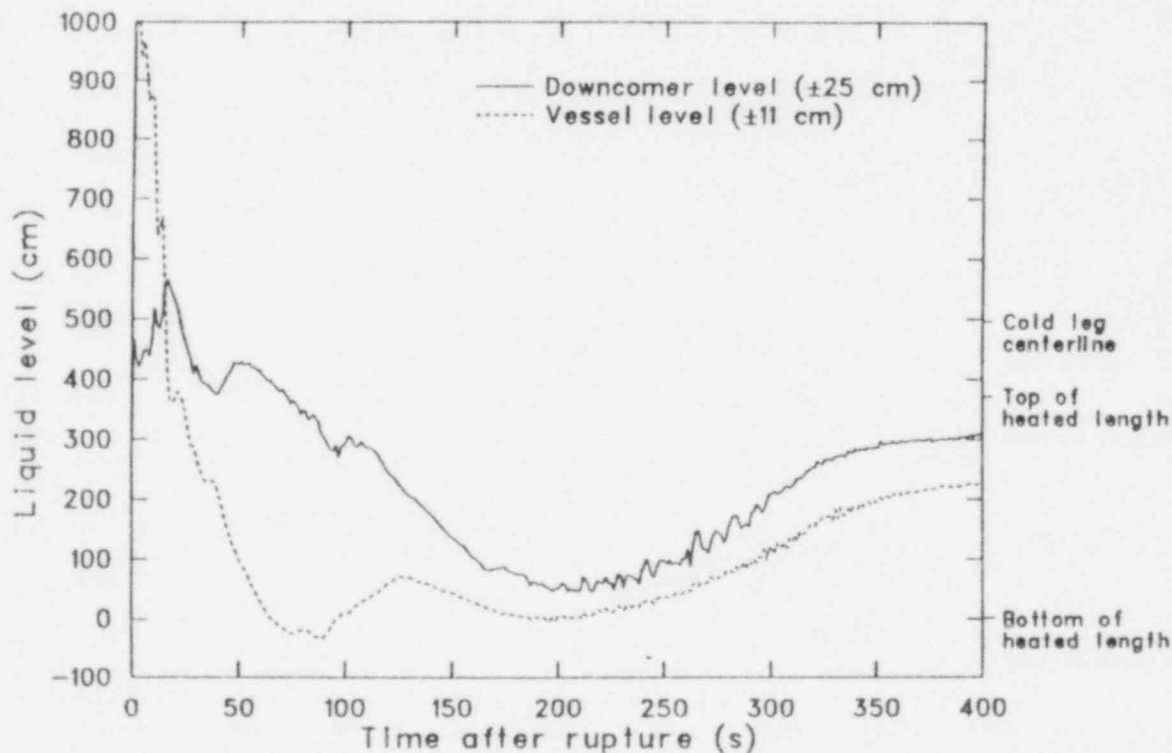


Figure 7. Vessel and downcomer collapsed liquid levels during the 21.7% break test (S-1B-3).

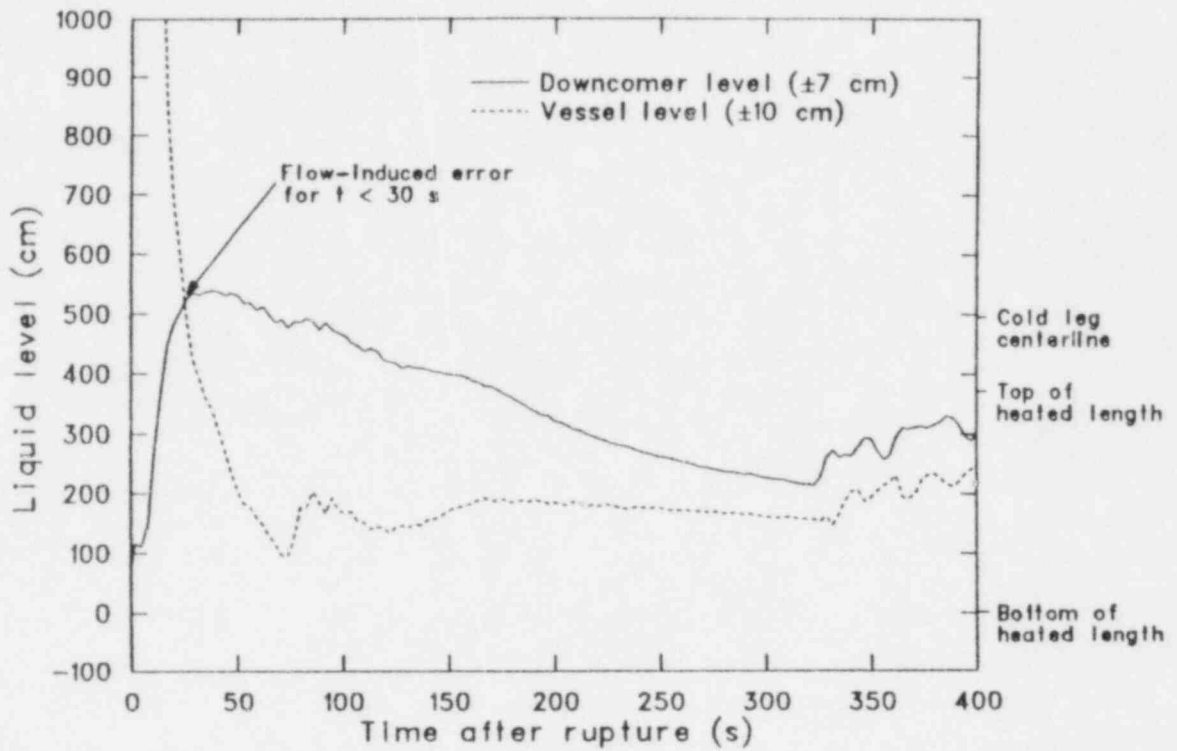


Figure 8. Vessel and downcomer collapsed liquid levels during the 10% break test (S-UT-1).

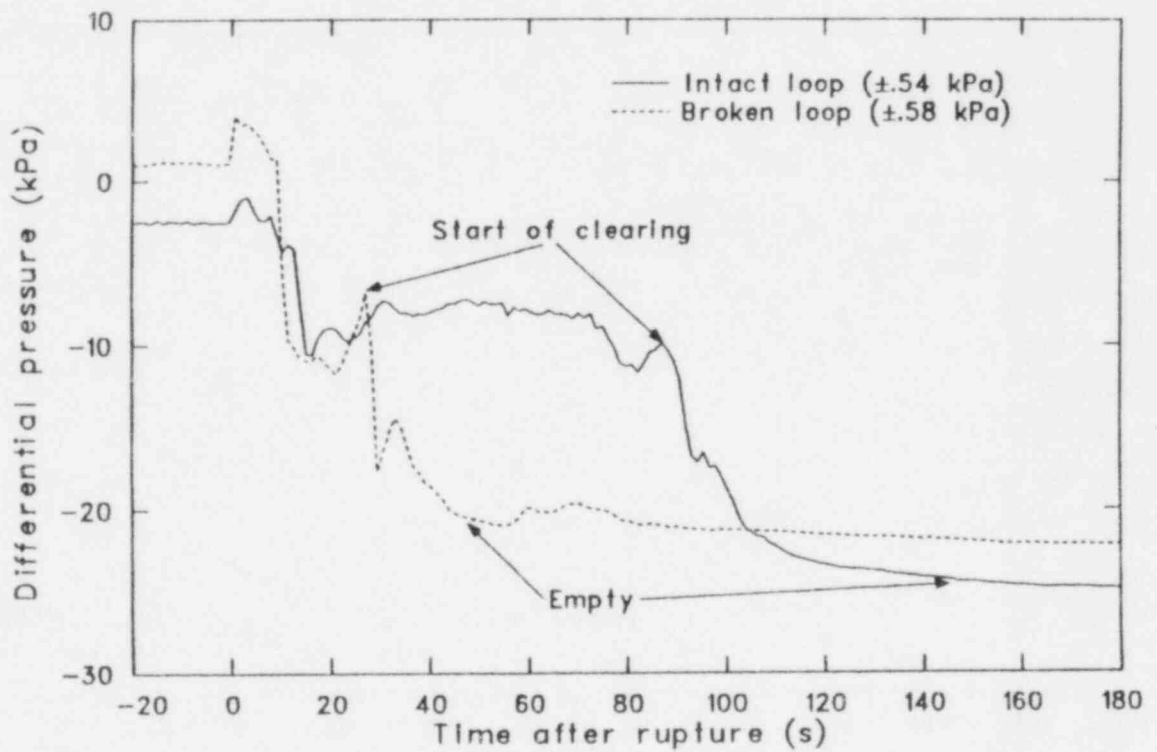


Figure 9. Pump suction upflow leg differential pressures (indicative of liquid levels) during the 21.7% break test (S-IB-3).

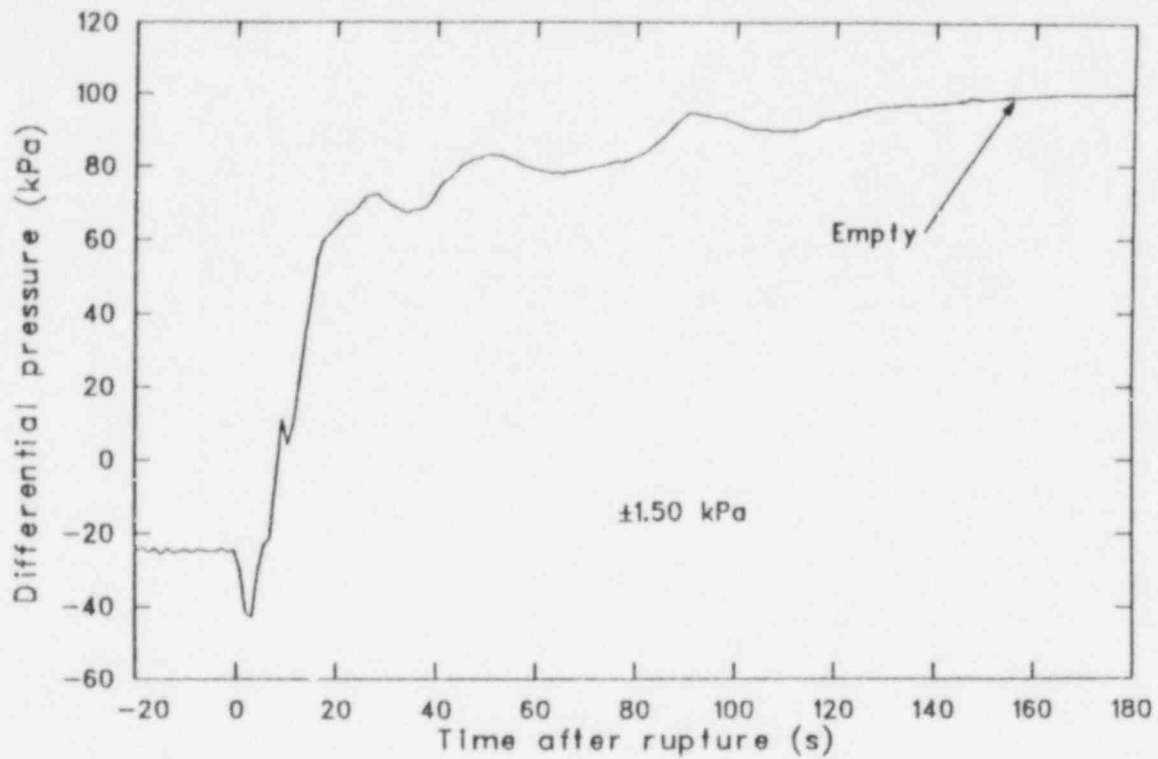


Figure 10. Intact loop steam generator U-tube upflow side differential pressures (indicative of liquid level) during the 21.7% break test (S-IB-3).

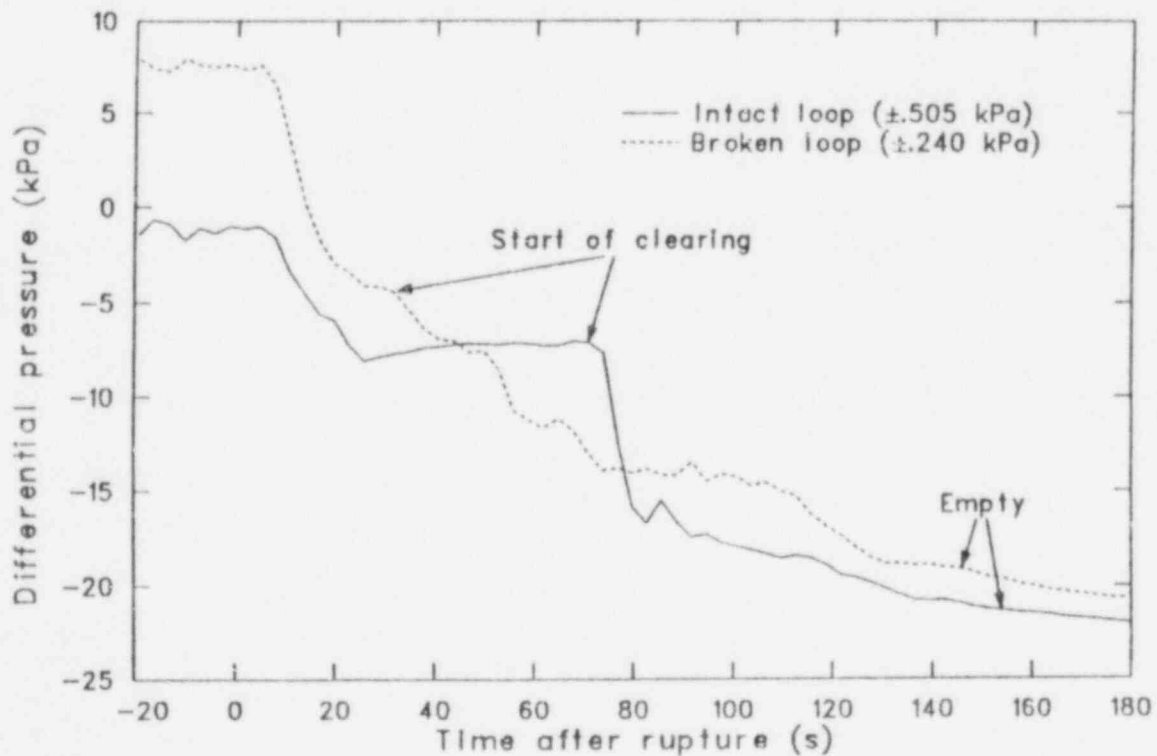


Figure 11. Pump suction upflow leg differential pressures (indicative of liquid level) during the 10% break test (S-UT-1).

pump suction is shown in Figure 8 as a recovery of the vessel level, to approximately the level of the pump suction, between 72 and 90 s. However, as shown in Figure 12, some liquid was being held up in the broken loop steam generator tubes until 140 to 150 s. The U-tube liquid gravity head, combined with that of the broken loop pump suction, caused the vessel level to continue to depress after the intact loop pump suction cleared. The vessel level depression continued until sufficient pressure buildup occurred in the vessel and broken loop hot leg to achieve the necessary pressure differential between the hot and cold legs to clear the broken loop steam generator U-tubes and pump suction. As shown in Figure 8, the manometric imbalance between the vessel and downcomer decreased as the broken loop pump suction and steam generator U-tubes cleared, and the vessel level recovered between 120 and 160 to 170 s. Slow boiloff of core coolant caused the vessel level to decrease between 170 and 330 s, at which time ECC accumulator liquid penetrated the downcomer and reflooding of the core was initiated.

The observed hydraulic responses in the vessel during the 10 and 21.7% break tests were very

similar, with only minor differences being noted, i.e., which of the two loops determined the final vessel level recovery and the extent of the vessel level depression. The larger broken loop flow rate observed during the 21.7% break test is believed to have caused the broken loop pump suction to clear earlier than during the 10% break test. Also, the intact loop steam generator was allowed to steam until the primary system pressure reached 1 MPa during the 21.7% break test, whereas the intact loop steam generator was isolated at blowdown during the 10% break test. The decreasing pressure in the intact loop steam generator during the 21.7% break test provided lower secondary fluid temperatures than would have occurred had the steam generator been isolated at blowdown. This in turn allowed a longer period of condensation to occur in the primary side of the U-tubes. This longer condensation period caused the U-tube liquid gravity head to be greater, which, when combined with the pump suction liquid gravity head, caused the manometric imbalance between the vessel and downcomer to be greater. Thus, the extent of the vessel level depression was greater during the 21.7% break test than during the 10% break test,

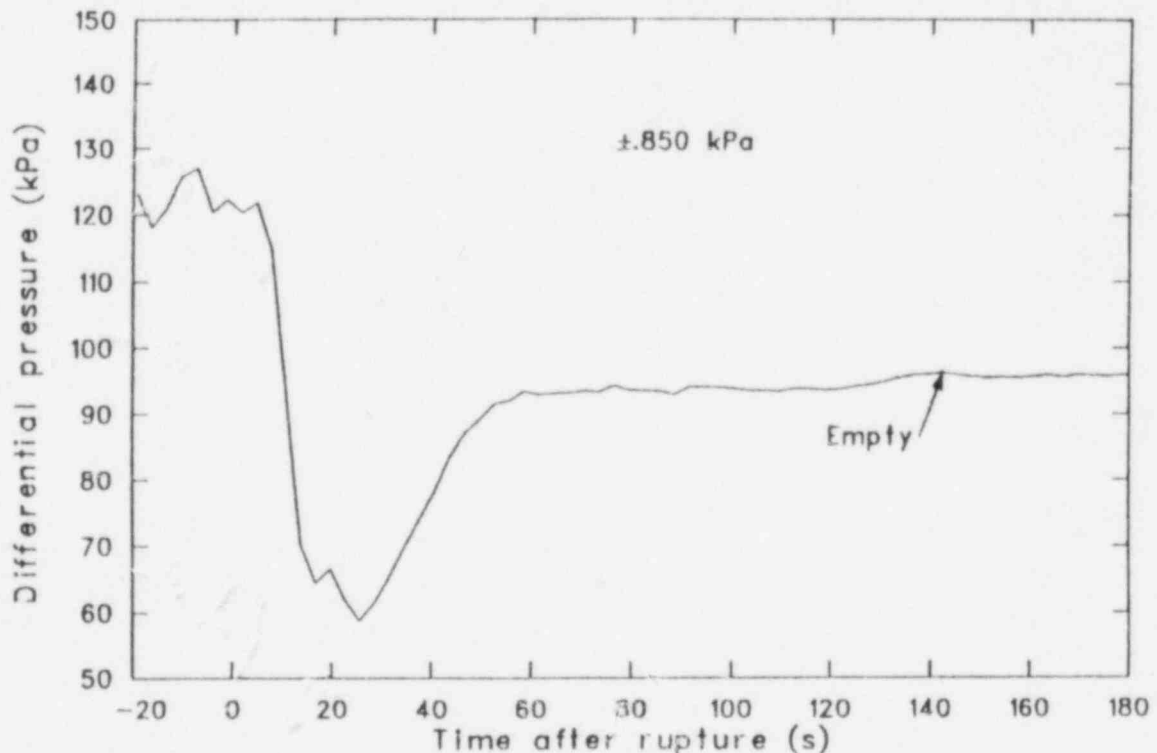


Figure 12. Broken loop steam generator U-tube upflow side differential pressures (indicative of liquid level) during the 10% break test (S-UT-1).

due in part to the allowed depressurization of the intact loop steam generator. Reference 11 provides a more detailed analysis of the effects of steam generator behavior on core coolant level depression during small breaks in the Semiscale system.

The trends of the primary system depressurizations during the 200, 100, and 50% break tests are very similar, as shown in Figure 13. The upper plenum fluid reached saturation conditions almost immediately after rupture of the pressure boundary during all three tests. The effect of this is shown in the figure as the first decrease in the depressurization rates. As the system continued to depressurize, the effect of the entire system reaching saturation conditions can be seen as the second decrease in the depressurization rates. The depressurizations continued to be rapid, due to the previously discussed large break flow rates, and the system was voided rapidly during the transients. The system pressure reached containment simulator pressure within 105 s after rupture of the pressure boundary during all three tests. This rapid depressurization of the primary system caused early decoupling of the primary and secondaries. Hence, primary-to-secondary heat transfer was unimportant to system energy

removal during the transients. The primary energy removal mechanisms were the large break mass flows.

The trends observed during the depressurization of the primary system during the 21.7 and 10% break tests are very similar. As shown in Figure 14, the changes in the depressurization rates due to the occurrence of saturation conditions are quite similar. After reaching system saturation, the depressurizations proceed at a substantially reduced rate and at a pressure somewhat above secondary pressures. During both tests, containment simulator pressures were not reached until at least 240 s after rupture of the pressure boundary. The slow depressurization of the primary system after system saturation allowed primary-to-secondary heat transfer to contribute to system energy removal until 150 to 160 s after rupture of the pressure boundary.

In summary, the hydraulic responses of the 100 and 50% intermediate break tests were very similar to that of the 200% large break test. Also, the hydraulic response of the 21.7% intermediate break test was very similar to that of the 10% small break test.

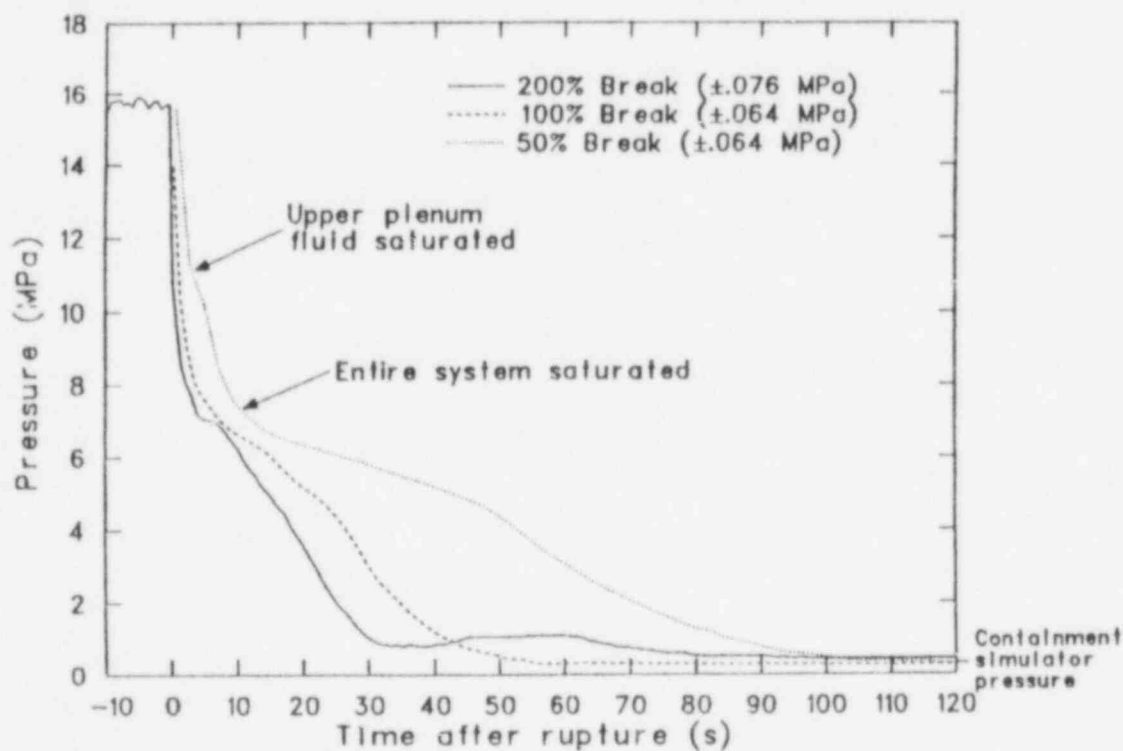


Figure 13. Primary system vessel upper plenum pressures during the 200, 100, and 50% break tests.

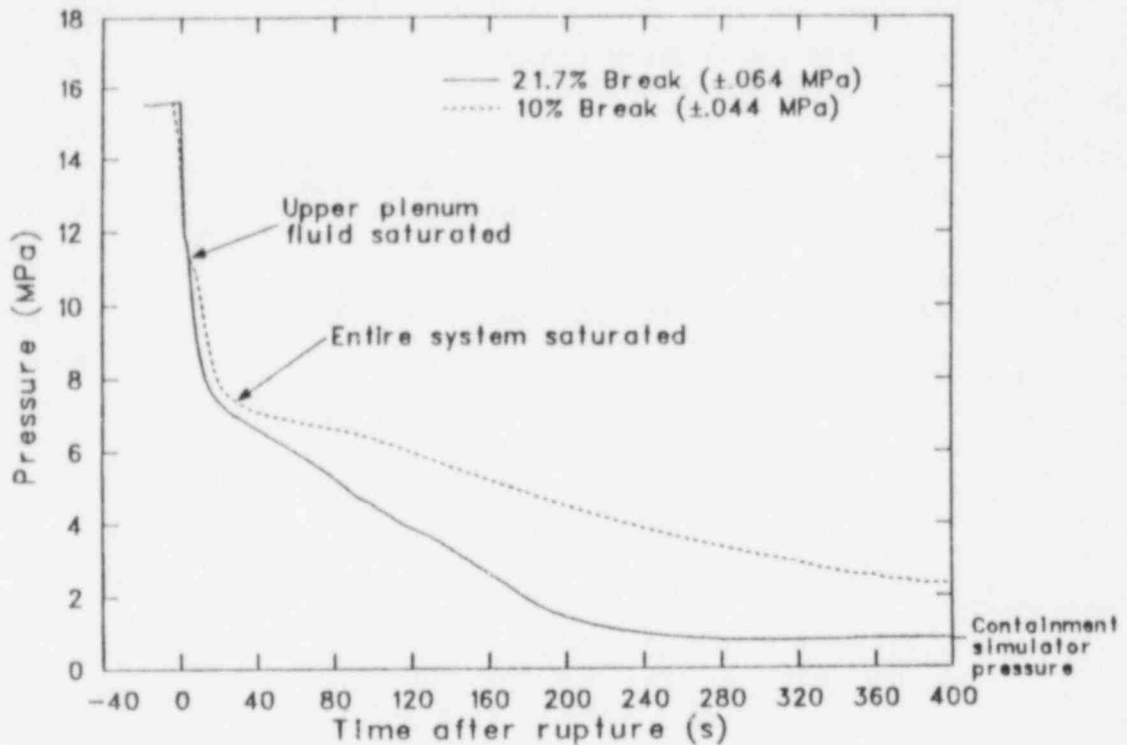


Figure 14. Primary system vessel upper plenum pressures during the 21.7 and 10% break tests.

3.2.3 Thermal Response During Large, Intermediate, and Small Breaks. The thermal response in the core after rupture of the pressure boundary was very similar during the 200 and 100% break tests. As shown in Figure 15, the heater rods experienced very severe temperature excursions. This was due to departure from nucleate boiling occurring at the heater rod surfaces while the rods had a high level of stored energy. The elevated temperatures continued as voiding in the core increased while the stored energy in the rods was being dissipated. As the rods reached decay heat power levels at about 20 s, the heater rod temperatures started to decrease.

As discussed in Section 3.2.2, the ECC accumulator started injecting into the vessel lower plenum at about 20 s after rupture of the pressure boundary during the 200% break test. This precipitated an immediate refill of the vessel lower plenum and initiated reflooding of the core, which was continued by scaled, LPIS flow. Thus, as the level rose in the core, the cooling effect of the generated steam was sufficient to decrease heater rod temperatures and eventually quench the rods as low quality steam and water droplets reached their surfaces.

During the 100% break test, as discussed in the previous section, the amount of ECC accumulator liquid that was bypassed to the break was excessive compared to that expected for a PWR. This caused the refilling of the vessel lower plenum to be atypically driven by only a degraded LPIS flow and caused the reflooding of the vessel to be atypically slow due to the degraded LPIS flow. Thus, as the vessel level fell and the steam flow decreased, the heater rod temperatures started to increase again at about 40 s after rupture of the pressure boundary. The slow reflooding of the vessel caused high quality, low flow conditions to exist in the core for an extended period. Although elevated temperatures still existed in the core at the end of data acquisition time, they had reached a plateau and started to decrease. The slowly increasing vessel level was producing sufficient steam to afford some cooling of the rods. Although a quench of the rods did not occur prior to the end of data acquisition time, the rising vessel level and decreasing temperatures indicate that a quench was imminent.

The thermal response in the core immediately after rupture of the pressure boundary was similar during the 50, 21.7, and 10% break tests. As shown in Figure 16, the heater rods did not

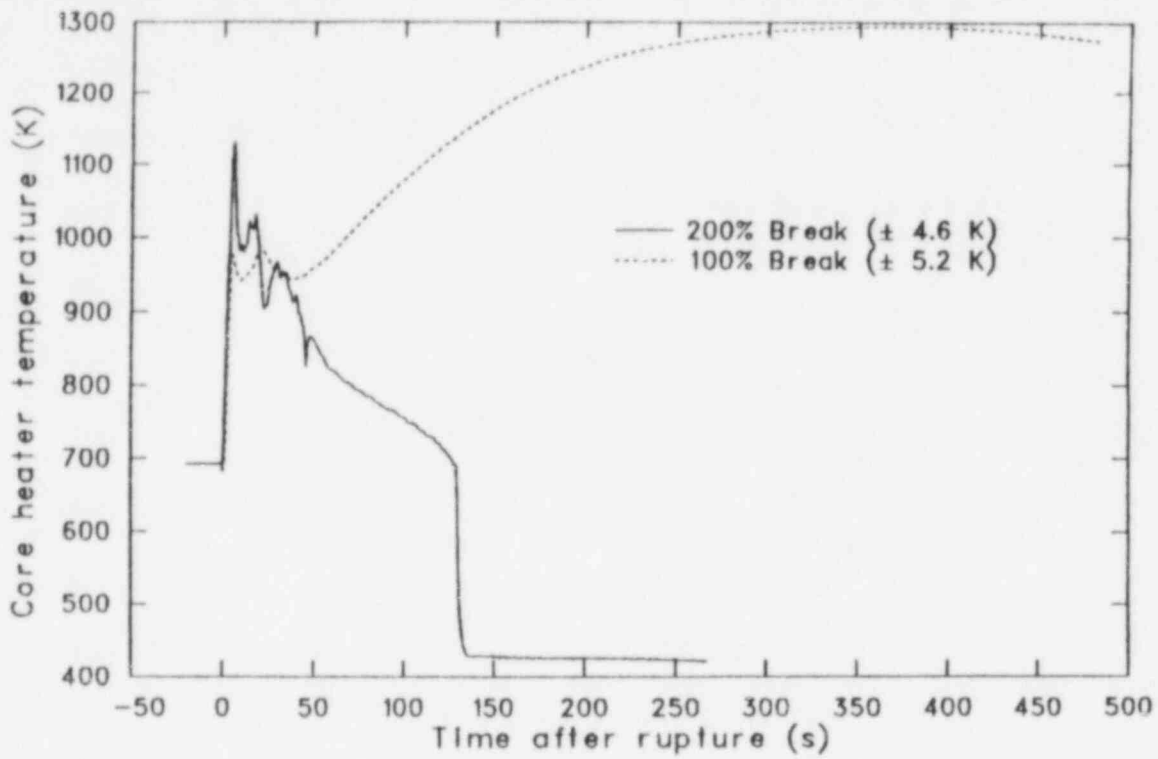


Figure 15. Peak heater rod temperatures during the 200 and 100% break tests.

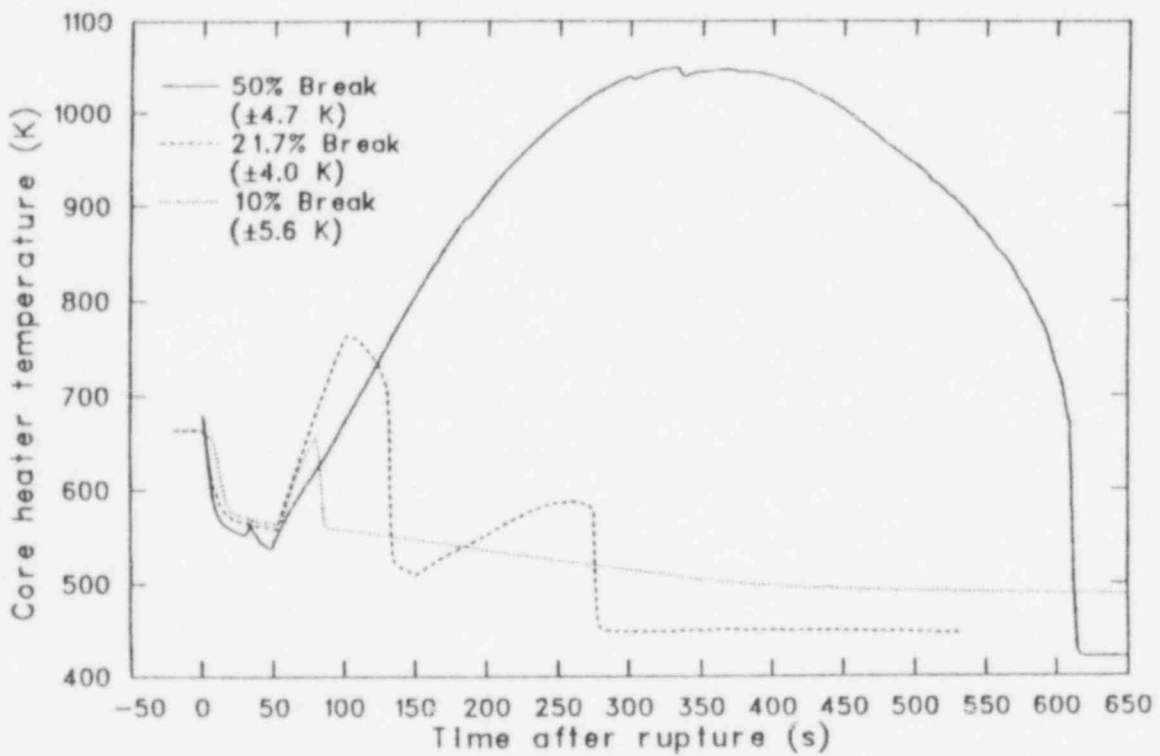


Figure 16. Peak heater rod temperatures during the 50, 21.7, and 10% break tests.

experience temperature excursions until the rods were at decay heat levels. The elevated temperatures were caused by the existence of low velocity, high quality conditions in the core, which lead to dryout of the heater rod surfaces.

During the 50% break test, as discussed in Section 3.2.2, the relatively large mass flow rates did not leave the vessel devoid of coolant until about 40 s after rupture of the pressure boundary. Thus, the voiding in the core was slow enough to provide sufficient cooling of the heater rods while they had a high level of stored energy, and the thermal response of the core was initially similar to the response of the 10 and 21.7% break tests. The vessel remained devoid of coolant from 40 s after rupture of the pressure boundary until reflood was initiated. Additionally, an excessive amount of bypass of ECC accumulator liquid to the break occurred during the 50% break test, similar to the 100% break test. This caused vessel reflooding to be delayed and initiated by only the degraded LPIS flow. Thus, since the level in the vessel remained near the bottom of the core, the low flow, high quality conditions continued to exist in the core. This continued until the fluid in the vessel reached a level sufficient to allow low quality steam and water droplets to reach and rewet the surface of the rods. Consequently, the thermal response in the core after 40 s was similar to the response observed during the 100 and 200% break tests.

The existence of intact loop pump suction and steam generator U-tube liquid seals caused a level depression in the vessel during the 21.7% break test, as discussed in Section 3.2.2. This depressed level in the vessel caused low flow, high quality conditions to exist in the core and led to the first temperature excursion observed during this test. The temperature excursion continued until the intact loop pump suction and steam generator U-tubes had cleared enough to allow the vessel level to recover, and increased flow of lower quality steam reached and rewet the surfaces of the heater rods. After the level in the vessel recovered, slow boiloff of coolant caused the level in the vessel to decrease. As the level neared the bottom of the core, low flow, high quality conditions reoccurred and dryout of the heater rods led to a second temperature excursion. This second temperature excursion continued until the core was sufficiently reflooded to cause the rods to rewet.

As discussed in Section 3.2.2, the existence of intact and broken loop pump suction and steam generator U-tube liquid seals caused a level depression in the vessel during the 10% break test. This depressed level in the vessel caused low flow, high quality conditions to exist in the core and led to the first temperature excursion of the test. This temperature excursion continued until the intact loop pump suction and steam generator U-tubes partially cleared and allowed the level in the vessel to partially recover, thus, allowing low quality steam and water droplets to reach and rewet the surface of the rods. After the partial level recovery in the vessel, the level depressed again, although less severely, due to the broken loop pump suction and steam generator U-tube liquid seals. The peak heater rod temperature, shown in Figure 16, did not indicate another dryout because the continued level depression was less severe than that which occurred before partial recovery. However, higher rod elevations experienced a second, small temperature excursion which continued until the broken loop pump suction and steam generator U-tubes cleared enough to allow the vessel level to recover, thus rewetting the surfaces of the heater rods. Slow boiloff of core coolant, after level depression recovery, did not deplete enough coolant to allow a third temperature excursion before vessel reflooding was initiated.

In summary, the core thermal responses during the 100% intermediate break test and the 200% large break test were very similar, as were the responses during the 21.7% intermediate break test and the 10% small break test. Although the thermal response during the 50% intermediate break test was similar to those during the 21.7 and 10% break tests up to 40 s after rupture, the response after that time was similar to those during the 100 and 200% break tests.

3.3 Comparison of Semiscale and LOFT Intermediate Break Data

The typicality of Semiscale intermediate break test data is addressed in the following sections. The response observed during an intermediate break experiment performed in the Loss-of-Fluid Test (LOFT) facility is compared with that observed during Semiscale intermediate break (21.7%) Test S-IB-3. Comparison of the results

from the two facilities aids in evaluating the validity of the scaling philosophy applied to the facility designs, as well as lending credence to the usefulness of the test results for code assessment purposes.

The LOFT intermediate break Test L5-1^{12,13} simulated a break in the cold leg of a commercial PWR between the downcomer inlet and pump, with a scaled break area representing approximately 21% of the area of the cold leg of a commercial PWR. Briefly, the LOFT system is a 50-MW(t) PWR, consisting of a reactor vessel with a nuclear core, an intact loop, and a broken loop. The intact loop contains an active steam generator, pressurizer, and two primary coolant pumps in parallel. The broken loop contains a simulated steam generator, simulated pump, and two quick-opening blowdown valve assemblies. Similar to Semiscale, the blowdown pressure suppression system consists of a header, suppression tank, and a spray system. The ECC injection system consists of two LPIS pumps, two HPIS pumps, and two accumulators.

A brief discussion of the results of a comparison of the hydraulic and thermal responses of the two tests follows.

3.3.1 Comparisons of Thermal-Hydraulic Responses During Semiscale Test S-IB-3 and LOFT Test L5-1. The primary system depressurizations during the two tests showed similar trends. However, as shown in Figure 17, the rates of the depressurizations were slightly different during most of the transient. This was due to slight differences in break size and initial fluid conditions, as well as differences in the buildup of pressure in the vessel upper plenum associated with loop seal formation. The volume of the LOFT upper plenum and hot legs represents about 10.6% of the total system volume, whereas the volume of the Semiscale upper head, upper plenum, and hot legs represents about 14.7% of the total. Upon reaching saturation, the upper plenum and hot leg fluid volume acts as a "pressurizer." The smaller relative "pressurizer" volume in LOFT allows the system to depressurize faster than the Semiscale system. Thus, the effect

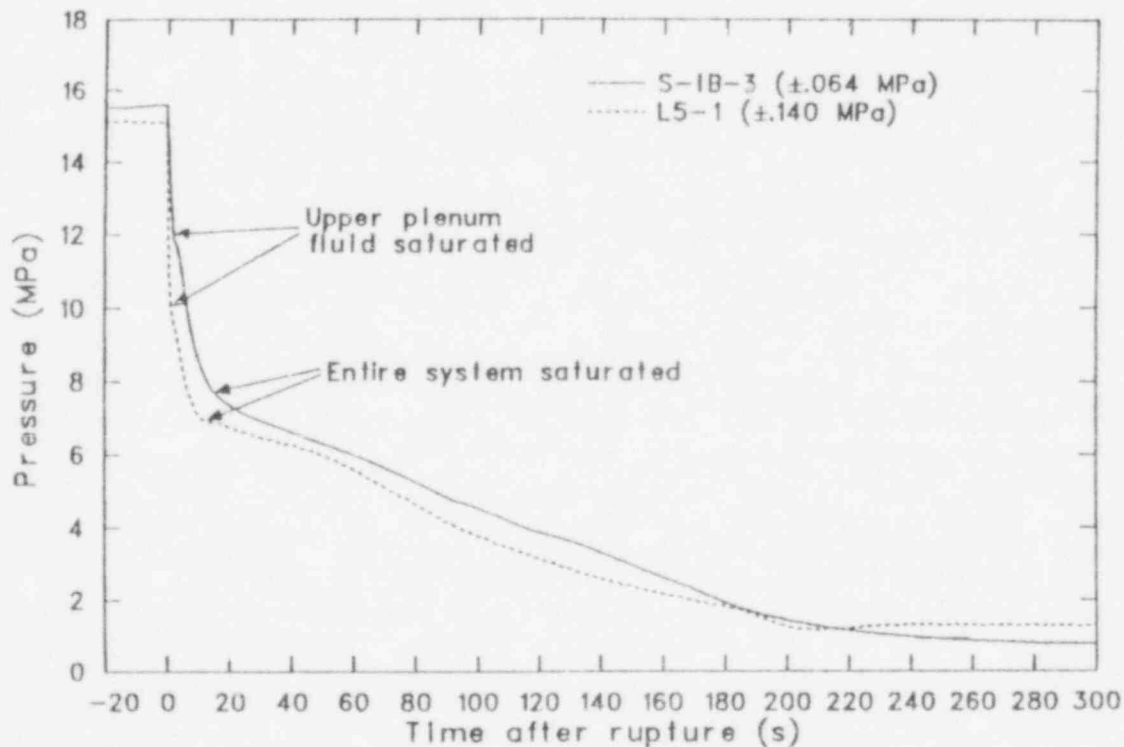


Figure 17. Primary system vessel upper plenum pressures during Semiscale Test S-IB-3 and LOFT Test L5-1.

on the depressurization of the vessel upper plenum and the hot leg fluid reaching saturation conditions is more pronounced in Semiscale than it is in LOFT. Hence, the first decrease in the rate of the depressurization was greater during Test S-IB-3 than during Test L5-1. Also, as shown in Figure 17, the faster depressurization during Test L5-1 caused the LOFT system to reach saturation conditions earlier than did the Semiscale system. The differences in the timing of the second

depressurization rate decrease are due to differences in reaching system saturation during the two tests. Colder initial fluid temperatures cause a lower system saturation temperature and pressure. As shown in Table 3, the LOFT hot and cold leg fluid was initially colder than that in Semiscale. This caused the LOFT system to reach saturation conditions at a lower pressure during Test L5-1 than did the Semiscale system during Test S-IB-3, as shown in Figure 17.

Table 3. Initial conditions for Tests S-IB-3 and L5-1

	<u>S-IB-3</u>	<u>L5-1</u>
Primary Coolant System		
Hot leg pressure (MPa)	15.55	14.93
Cold leg temperature (K)		
Intact loop	559.4	552.3
Broken loop	566.4	549.2
Hot leg temperature (K)		
Intact loop	596.1	579.3
Broken loop	596.9	554.3
Core temperature rise (K)		
Intact loop	36.7	27.0
Broken loop	30.5	NA
Total core power (MW)	1.45	45.9
Total loop flow rate (kg/s)	7.99	308.2
Secondary Coolant System		
Steam generator secondaries pressure (MPa)		
Intact loop	6.48	5.05
Broken loop	7.53	NA
Coolant Injection System		
Intact loop accumulator		
Pressure (MPa)	2.6	1.66
Water volume (m ³)	0.066	2.25
Nitrogen volume (m ³)	0.015	1.59
Water temperature (K)	298	308

As discussed in Section 3.2.2, the vessel level was depressed during Test S-IB-3 due to intact loop liquid seal formation. Since the depressed liquid level in the vessel is caused by the loop seal formed by liquid in the pump suction, the depth of the vessel liquid prior to loop seal clearing is directly related to the gravity head of the liquid in the pump suction. Thus, a shallower pump suction (LOFT's is much shallower than Semiscale's) will require less of a differential pressure across it to cause the liquid to be cleared. Correspondingly, the smaller differential pressure across the pump suction also means a smaller differential pressure between the vessel and the downcomer. Therefore, the manometric imbalance between the vessel and downcomer is smaller, i.e., the level depression in the vessel is less severe. Thus, the shallower LOFT pump suction prevented the occurrence of a vessel level depression similar to that in Semiscale.

The area of the bypass flow path can also affect the occurrence and extent of level depression in the vessel, and the LOFT core bypass flow path has a larger relative area than does Semiscale. During the period of loop seal formation, the core bypass flow path becomes a primary means for steam generated in the core to exit the vessel. A larger relative flow area provides a lower relative resistance to flow, thus allowing higher flow rates through the flow path and providing greater capabilities for relieving the steam generated in the core. Consequently, the possibility of pressurization of the vessel due to steam buildup during the period of loop seal formation is minimized, which in turn decreases the possibility of the vessel level being depressed to the depth of the pump suction. Another means for steam relief in the LOFT vessel¹⁴ is via condensation on the large upper plenum metal structure and mixing of the resulting saturated liquid with the vessel coolant. This also tends to minimize the possibility of pressurization of the vessel due to steam buildup. Thus, the possibility of a depressed liquid level occurring in the LOFT vessel during Test L5-1, similar to that which occurred during Test S-IB-3, was also minimized by the large core bypass flow area, as well as condensation on the large upper plenum metal structure. Reference 11 provides a more detailed analysis of the effects of core bypass flow path on core coolant level depression.

Lack of sufficient data from Test L5-1 makes quantification of the separate effects of the large core bypass flow area and condensation on the large upper plenum metal structure impractical.

Although liquid level measurements were not available for Test L5-1, a comparison of the intact loop cold leg density measurements from the two tests, shown in Figure 18, provides evidence of the combined effect of the larger bypass flow area and the condensation on the large upper plenum metal structure in LOFT. Figure 18 suggests that the intact loop seal was clear by about 55 s during Test L5-1, as does Figure 19, which shows the fluid velocity in the intact loop cold leg. However, the Test L5-1 intact loop differential pressure between the hot leg vessel outlet and the cold leg vessel inlet indicates that the pressure differential across the pump suction was not sufficient to cause the loop seal to clear. As shown in Figure 20, the differential pressure was negligible after 12 s. This suggests that the core bypass flow path and the condensation on the upper plenum metal structure provided sufficient relief of the steam generated in the core to prevent a significant vessel level depression during Test L5-1. The clearing of the loop seal, therefore, was due to a hydrostatic draining of the pump suction as the voiding in the core lowered the vessel level past the depth of the shallow pump suction. Thus, the shallower pump suction, larger core bypass flow path, and condensation on the large upper plenum metal structure in LOFT prevented the occurrence of a vessel level depression similar to that in Semiscale.

Comparison of the Tests S-IB-3 and L5-1 calculated break mass flow rates, where the Test L5-1 mass flow has been divided by the volume scaling factor of 34.1, shows excellent agreement between the two tests. As shown in Figure 21, the flows followed the same trends of a sustained initial flow, followed by a gradual decrease as the fluid at the break changed from subcooled to saturated conditions.

The thermal response in the core during the two tests was determined by the core hydraulic response and by the core configuration. A depressed fluid level in the vessel can cause dryout of the cladding surfaces, followed by a rewet as the vessel level recovers. Subsequent boiloff of core coolant following vessel level recovery can also lead to a second dryout of the cladding surfaces, which will continue until reflooding of the vessel is accomplished. As discussed in Section 3.2.3, the Semiscale heater rods experienced two temperature excursions during Test S-IB-3. The first was due to the vessel level depression and the second was due to the boiloff of core

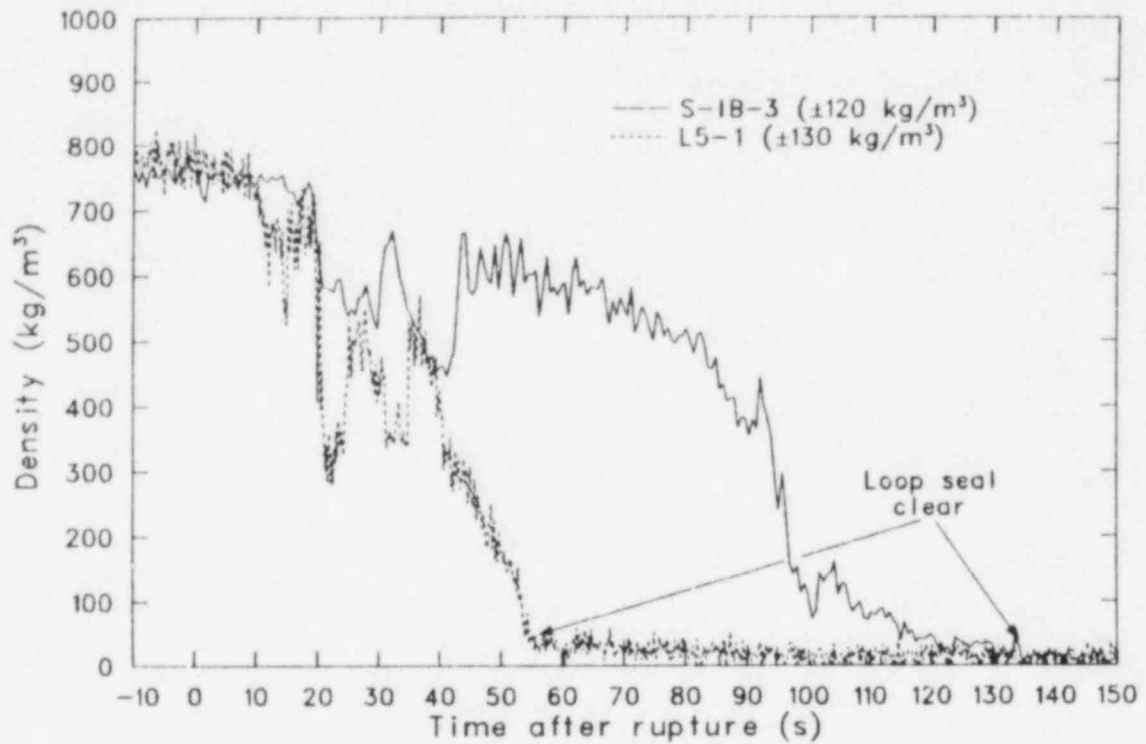


Figure 18. Comparison of intact loop cold leg densities during Semiscale Test S-IB-3 and LOFT Test L5-1.

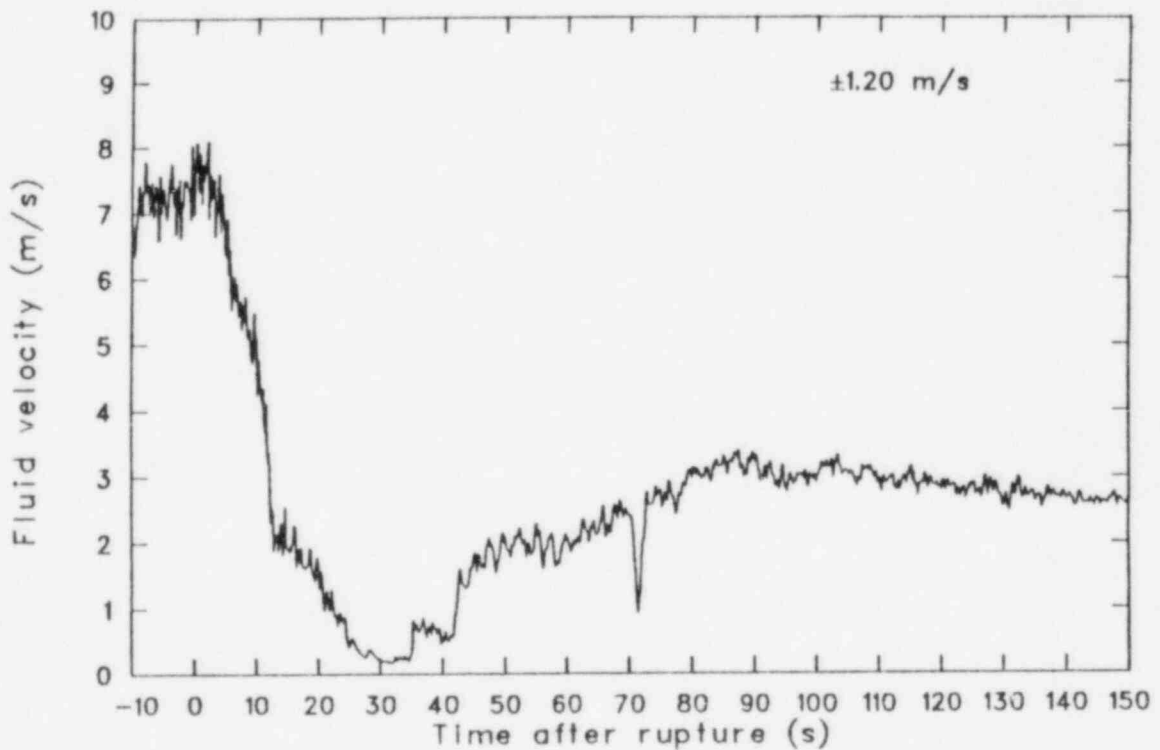


Figure 19. Intact loop cold leg fluid velocity during LOFT Test L5-1.

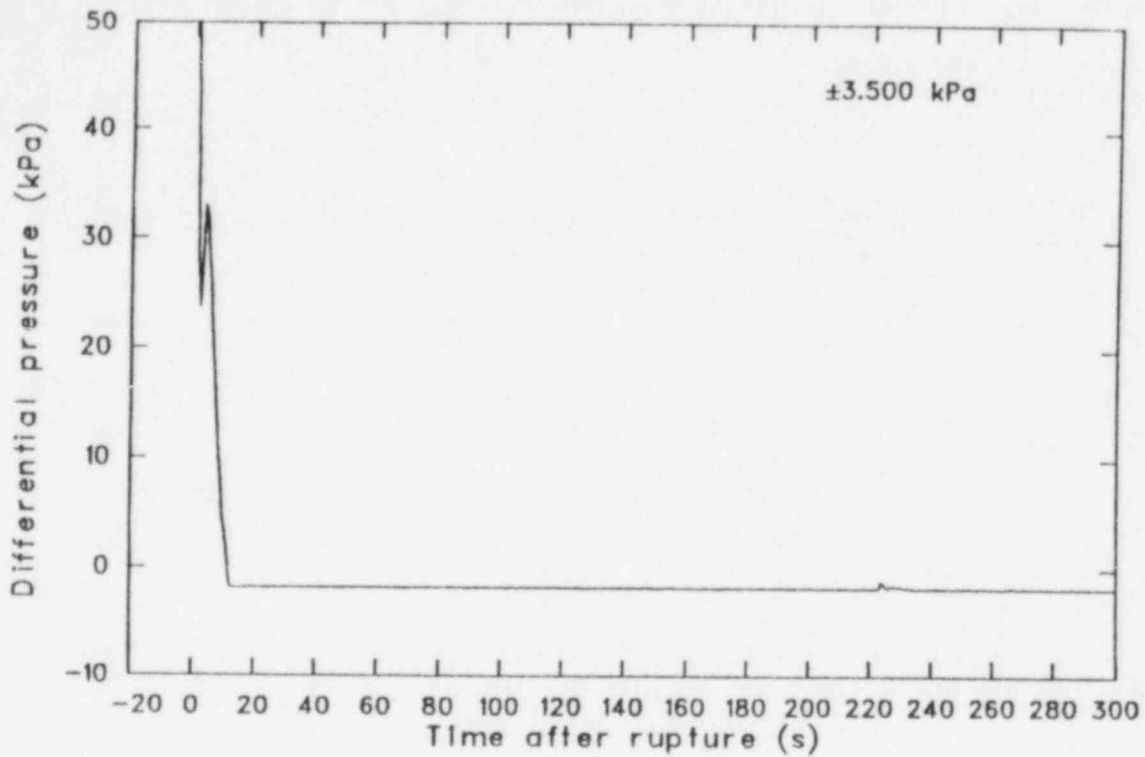


Figure 20. Intact loop differential pressure between hot leg vessel outlet and cold leg vessel inlet during LOFT Test L5-1.

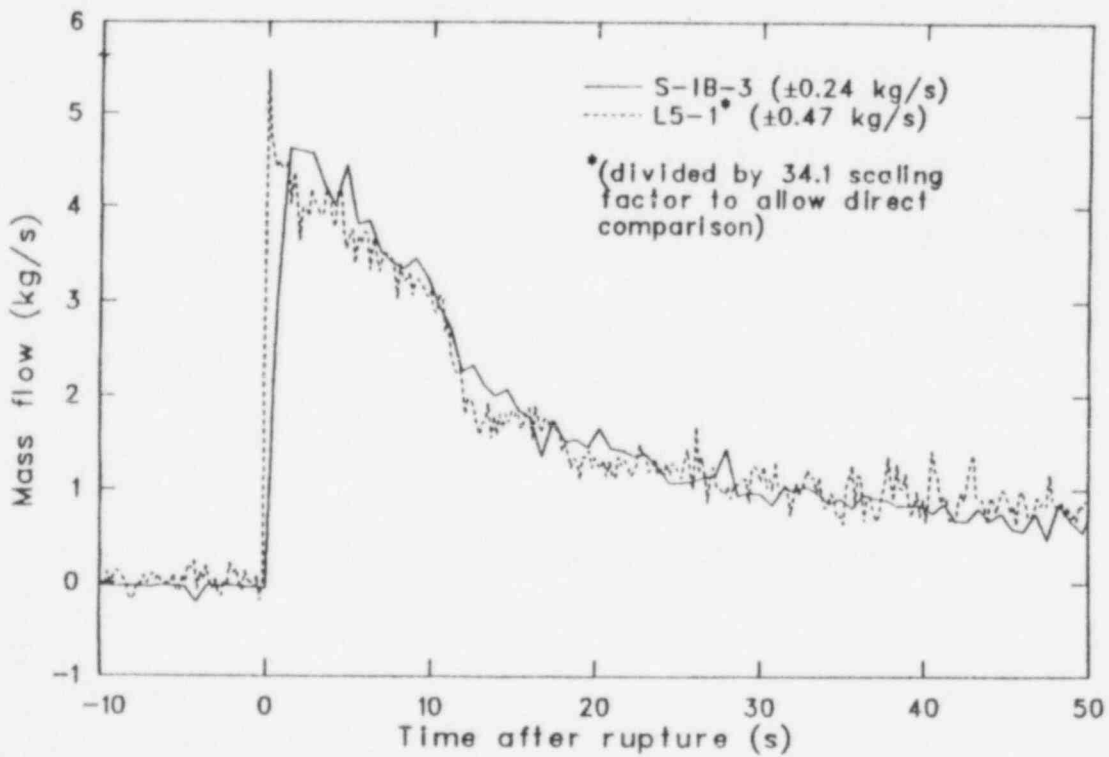


Figure 21. Comparison of break mass flow rates during Semiscale Test S-IB-3 and LOFT Test L5-1.

coolant. The LOFT nuclear rods experienced only one temperature excursion, which started at about 120 s, as shown in Figure 22, and was due to the boiloff of core coolant. As mentioned earlier, a vessel level depression in the LOFT facility similar to that observed in the Semiscale facility during Test S-IB-3 is precluded by the differences in system configurations.

The elevation of the top of the core can also affect the temperature response of the rod cladding. The lower positioning of the top of the LOFT core allows the cladding surfaces to remain wetted with a lesser amount of coolant in the core. Thus, the temperature excursion during Test L5-1 was also delayed, to a certain extent, due to the lower elevation of the top of the core. The thermal response of the core during Test L5-1, therefore, was influenced to a large degree by the greater core bypass flow path and the condensation on the large upper plenum metal structure, and to a lesser degree by the deeper positioning of the LOFT core. For these reasons, the LOFT and Semiscale core thermal responses were not in good agreement.

As discussed in Reference 13, the fuel cladding started to quench approximately 2.5 s after

accumulator injection began during Test L5-1. During Test S-IB-3, however, the excessive bypass of ECC coolant, caused in part by the Semiscale single-pipe downcomer, resulted in a delay of about 27 s between the initiation of accumulator injection and the initiation of vessel refilling.

In summary, some differences were noted in the hydraulic and thermal responses during the two tests. However, they were due to facility configuration differences rather than phenomenological differences. Although the period of the S-IB-3 transient during which the vessel level was depressed was not in agreement with the L5-1 test, the period of the transient following vessel level recovery showed the same trends during both tests.

3.4 Comparison of Semiscale and LOBI Intermediate Break Data

The Semiscale Mod-2A Intermediate Break Test Series included a counterpart test to one performed in the Loop Blowdown Investigation (LOBI) facility¹⁵ located in Ispra, Italy. The LOBI test, identified as B-R1M,^{3,16} simulated a

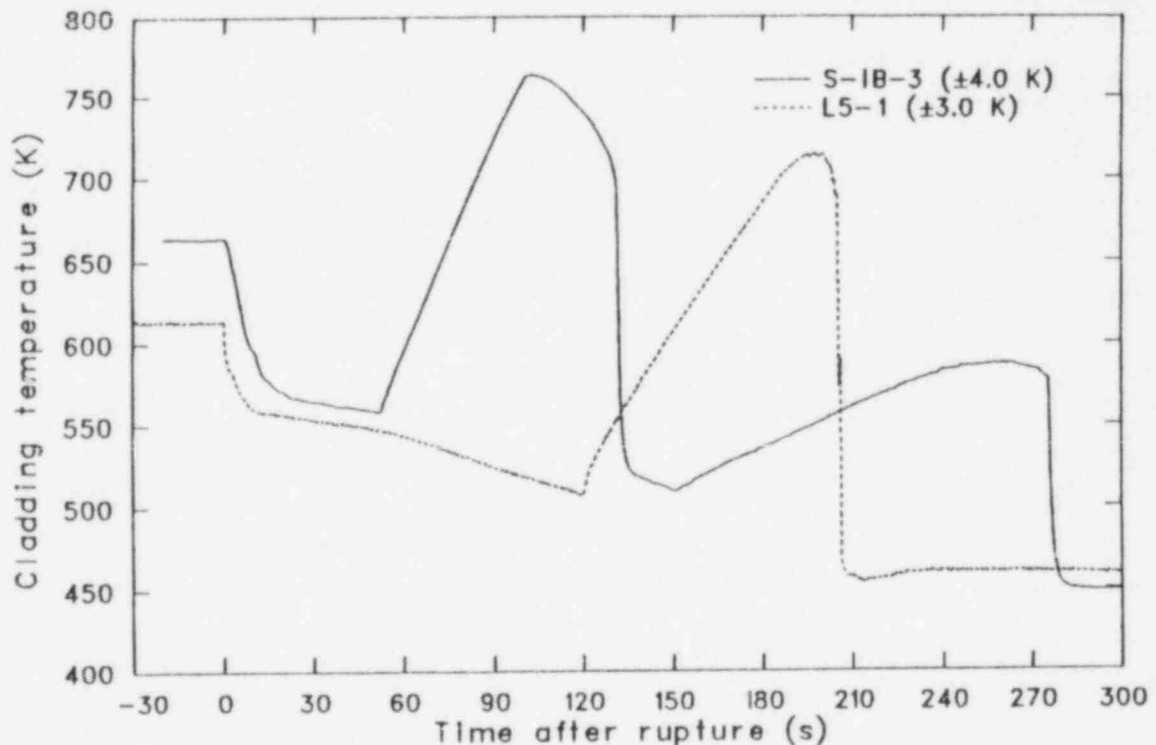


Figure 22. Comparison of peak heater rod temperature during Semiscale Test S-IB-3 and peak cladding temperature during LOFT Test L5-1.

25% break and was performed with a larger than scaled LOBI volume. Therefore, area-to-volume scaling to the Semiscale Mod-2A facility resulted in a 21.7% break test in Semiscale. The initial conditions and conduct of the Semiscale test, identified as S-IB-3, were chosen to be as similar as possible to those for the B-R1M test.

Briefly, the LOBI test facility simulates the primary cooling system of a four-loop, 1300-MW(e), German-designed KWU pressurized water reactor. The core power, primary coolant mass flow, and primary coolant volume were scaled down from the reactor values by a factor of 712. This led to a core power of 5.3 MW in the 8 x 8 electric heater rod bundle, a core mass flow rate of 28 kg/s, and a primary coolant volume of 0.82 m³. All of the other relevant parameters such as operating temperature and pressure, pressure drops, and lengths of heat transfer surfaces were scaled one-to-one. Also, the absolute heights and relative elevations of the individual system components were kept at reactor values, thus preserving the gravitational heads. Similar to Semiscale, the LOBI facility has an intact loop, which is scaled to simulate the three intact loops in a PWR, and a broken loop, which simulates the single loop in which a break is postulated to occur in a PWR. Both the intact and broken loops contain a main coolant pump and an active steam generator. Unlike Semiscale, the LOBI facility has an active secondary loop system containing two condensers, which simulate the reactor turbines, a cooler, and a feedwater pump. The emergency core cooling system for the B-R1M test consisted of only an intermediate pressure accumulator system.

Comparisons of the results of the two tests are important for several reasons. First, they provide a means of assessing the similarity of results obtained during nearly identical tests performed in the two facilities. Similarity in results over several scale sizes verifies the scaling philosophy applied to the facilities and lends credence to the usefulness of the results obtained by these facilities for code assessment purposes. Secondly, comparisons of the test results provide a means of investigating the characteristics peculiar to each of the facilities. Examination of the behavioral differences that occur between the systems highlights the significant roles certain configurational aspects have in influencing the test results.

The following sections describe the results of the data comparisons for the B-R1M and S-IB-3

tests. First, a comparison of the thermal-hydraulic responses during the two tests is presented for the purpose of assessing the similarity in test results for the two facilities. Subsequently, a discussion of the effects of facility configuration differences on test results is presented. In this way, differences in the test results that are attributable to the characteristics peculiar to each of the facilities are investigated. Finally, the effects of differences in test conduct on the test results are discussed.

3.4.1 Comparison of Thermal-Hydraulic Responses During Semiscale Test S-IB-3 and LOBI Test B-R1M. The depressurization of the primary system after rupture of the pressure boundary was very similar during the two tests. As shown in Figure 23, the rates of the depressurizations were almost identical during most of the transients. The occurrence of saturation in the vessel upper plenum is seen to have more of an effect on the depressurization in Semiscale than it does in LOBI. This is because the volume of the Semiscale upper head represents approximately 6.1% of the total system volume, whereas the volume of the LOBI upper head represents about 3.8% of the total system volume. This caused the first decrease in the rate of the depressurization to be greater during Test S-IB-3 than during Test B-R1M. As shown in Table 4, the intact loop cold leg fluid was initially warmer during Test B-R1M than during S-IB-3, which caused the cold leg fluid to reach saturation conditions earlier during Test B-R1M. Thus, the second reduction in the depressurization rate, associated with cold leg saturation, also occurred earlier during Test B-R1M. The slight disparities in the rates of the depressurizations, which occurred after the systems reached saturated conditions, were due to pressure buildup in the vessel upper plenum, associated with loop seal formation, occurring at different times during the two tests.

Comparisons of vessel and downcomer collapsed liquid levels during both tests indicate that the same general hydraulic response occurred in each of the vessels. As shown in Figure 24, the gravity-head-driven draining of the vessel and downcomer proceeded at a moderate rate, with a manometric imbalance occurring between the downcomer and vessel during both tests. As discussed in Section 3.2.1, the cause of the manometric imbalance during Test S-IB-3 was the formation of a liquid seal in the intact loop pump suction and steam generator U-tubes. This liquid seal cleared between 89 and 140 to 150 s, allowing the manometric imbalance to dissipate and the vessel level to recover.

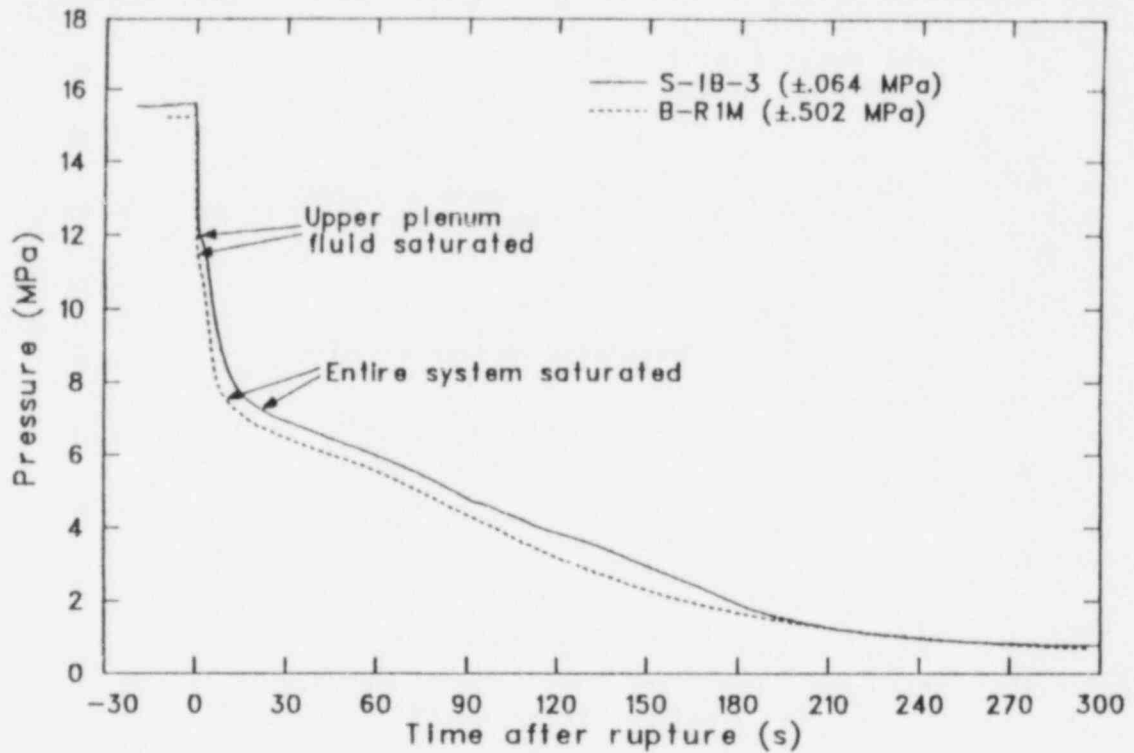


Figure 23. Primary system vessel upper plenum pressures during Semiscale Test S-IB-3 and LOBI Test B-R1M.

Table 4. Initial conditions for Tests S-IB-3 and B-R1M

	S-IB-3	B-R1M
Primary Coolant System		
Pressurizer pressure (MPa)	15.53	15.6
Upper plenum pressure (MPa)	15.58	15.5
Cold leg temperature (K)		
Intact loop	559.4	562
Broken loop	566.4	562
Hot leg temperature (K)		
Intact loop	596.1	593
Broken loop	596.9	599
Core temperature rise (K)		
Intact loop	36.7	31
Broken loop	30.5	37
Total core electrical power (MW)	1.45	5.19
Core inlet flow rate (kg/s)	7.69	26.04
Core bypass flow (% of total)	3.7	7
Secondary Coolant System		
Steam generator secondaries pressure (MPa)		
Intact loop	6.48	5.8
Broken loop	7.53	5.8
Coolant Injection System		
Intact loop accumulator		
Pressure (MPa)	2.6	2.6
Water volume (m ³)	0.066	0.224
Nitrogen volume (m ³)	0.015	0.056
Water temperature (K)	298	305

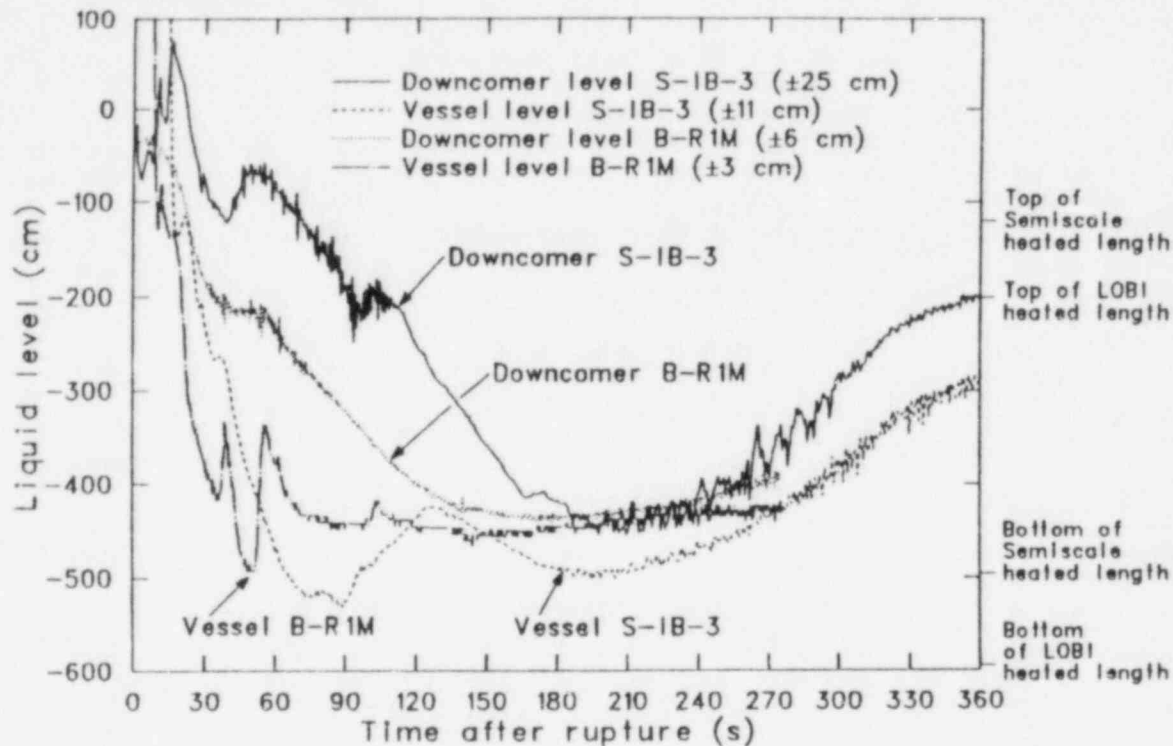


Figure 24. Comparison of vessel and downcomer collapsed liquid levels during Semiscale Test S-IB-3 and LOBI Test B-R1M.

Pump suction and steam generator U-tube differential pressure measurements were not available for Test B-R1M. However, comparisons of the intact loop hot and cold leg densities during the two tests, shown in Figures 25 and 26, indicate that the LOBI intact loop pump suction and steam generator U-tubes cleared between about 52 and 210 to 220 s. This coincides with the timing of the vessel level recovery observed in Figure 24 for the B-R1M test. Comparisons of the broken loop hot and cold leg densities during the two tests are inconclusive regarding the clearing of the LOBI broken loop pump suction. However, as shown in Figures 27 and 28, they do indicate that the LOBI broken loop pump suction and steam generator U-tubes were essentially cleared of liquid by about 45 to 50 s. Thus, the broken loop seal cleared before the intact loop seal during both tests. This caused the intact loop seal to control the extent and timing of the vessel level depression during both tests. Some of the reasons for the differences in the timing of the intact and broken loop seal clearings are discussed in Sections 3.4.2.3 and 3.4.3.

The manometric imbalance between the downcomer and vessel was more profound during the Semiscale test than during the LOBI test (Figure 24). The volume of the vessel and the downcomer will affect the extent of the manometric imbalance between the two. The vessel level depresses due to the gravity head of the liquid in the loop seal. The liquid volume transferred from the vessel to the downcomer, due to the depressed vessel level, causes a change in the downcomer liquid volume, which produces a corresponding change in the downcomer liquid level. Thus, the effect of the depressed vessel level on the downcomer liquid level is determined by the volume of the vessel and the downcomer. Although the Semiscale downcomer and vessel volumes and the LOBI vessel volume were correctly scaled, the LOBI downcomer volume was larger than scaled. The larger relative LOBI downcomer volume caused the change in downcomer liquid level, due to the volume of the displaced vessel liquid, to be less prominent. Therefore, the manometric imbalance between the vessel and downcomer was also less prominent during the LOBI test.

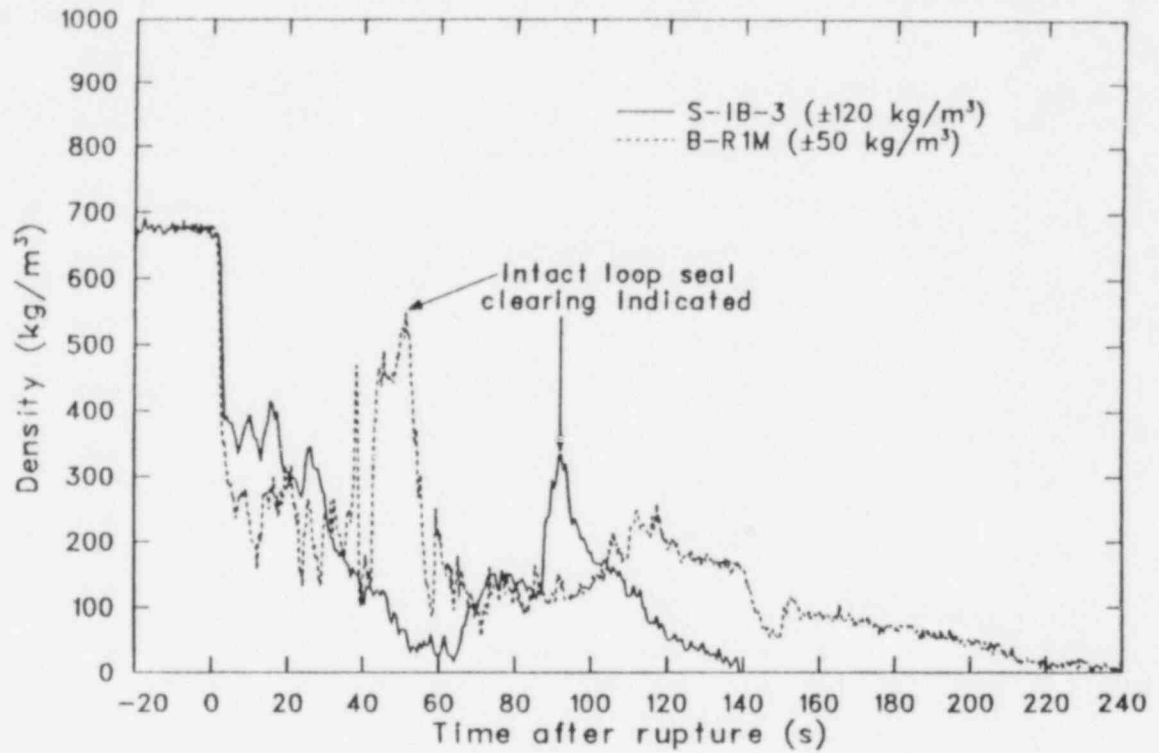


Figure 25. Comparison of intact loop hot leg densities during Semiscale Test S-IB-3 and LOBI Test B-R1M.

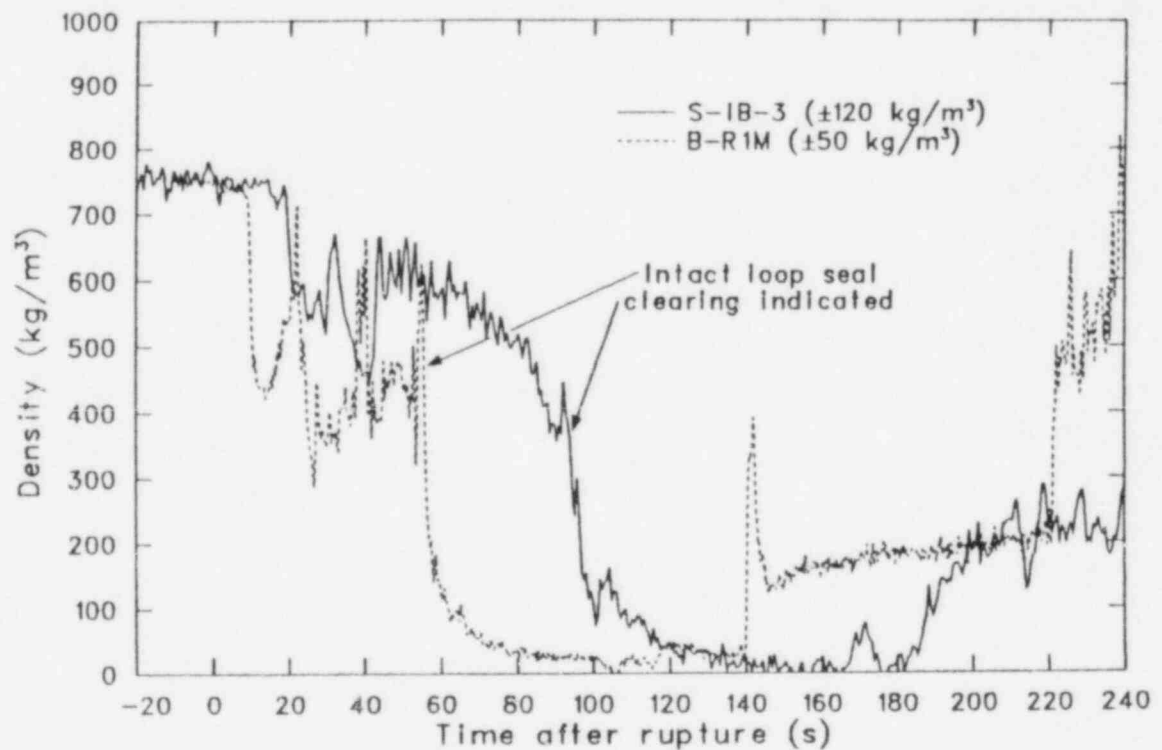


Figure 26. Comparison of cold leg densities during Semiscale Test S-IB-3 and LOBI Test B-R1M.

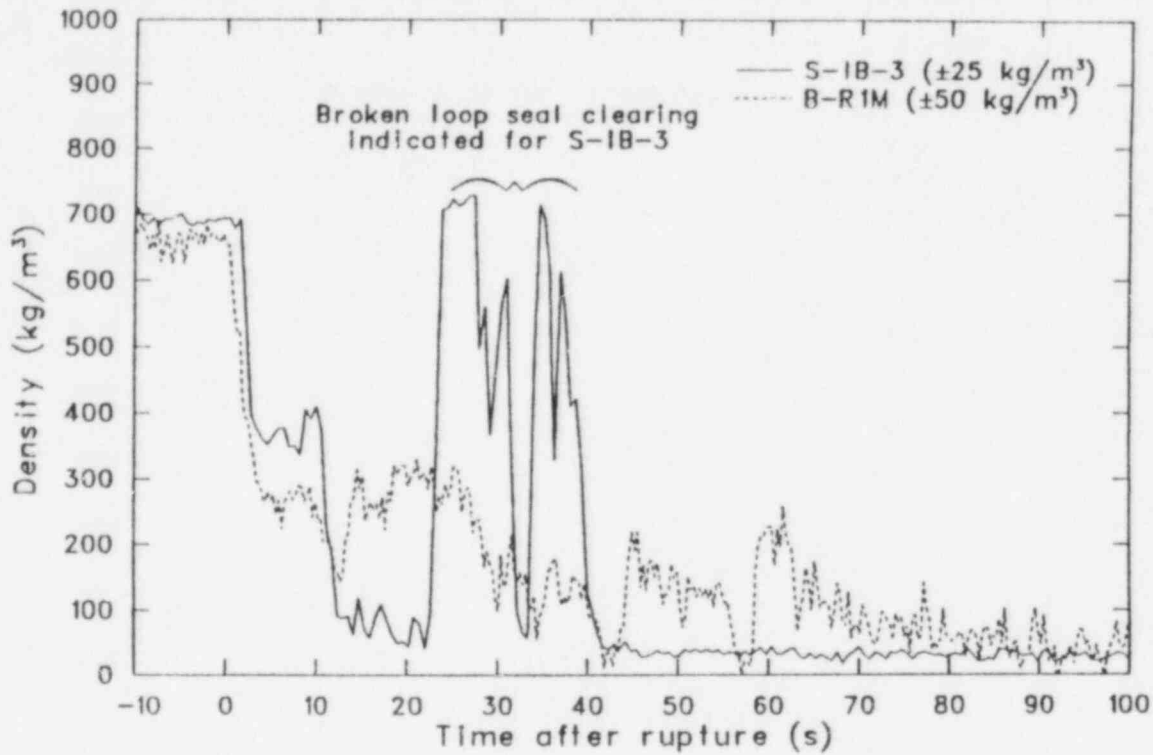


Figure 27. Comparison of broken loop hot leg densities during Semiscale Test S-IB-3 and LOBI Test B-R1M.

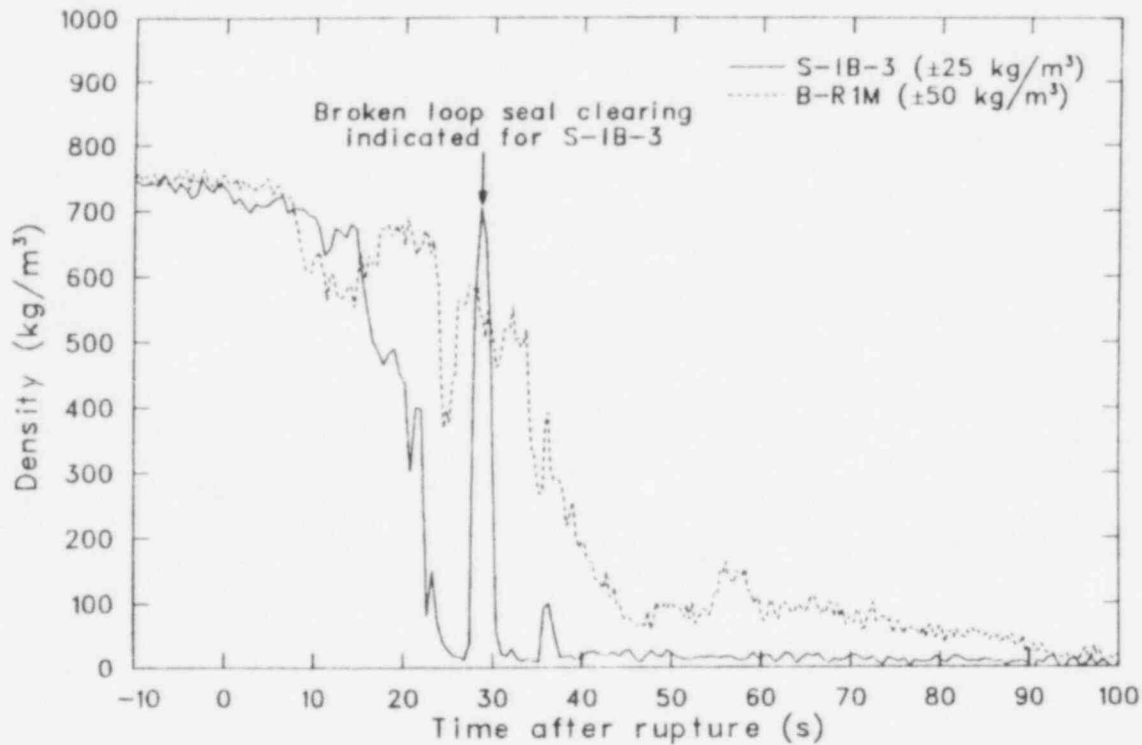


Figure 28. Comparison of broken loop cold leg densities during Semiscale Test S-IB-3 and LOBI Test B-R1M.

Comparisons of the calculated break mass flow rates during the two tests^a indicate that the initial break flow behaviors were very similar. As shown in Figure 29, the flows followed the same trend of a sustained initial flow, followed by a gradual decrease as the fluid at the break changed from subcooled to saturated conditions. (The method of calculating the break flow rates and the uncertainties in the flow measurements cause the unrealistic negative break flow values shown in the figure. Also, uncertainties in the Semiscale and LOBI break flow measurements make the comparisons of the flow rates for the two tests impractical after about 10 s following rupture of the pressure boundary.)

The thermal responses in the core during the two tests were quite dissimilar, as shown in Figure 30. The LOBI heater rods did not experience any temperature excursions during the B-R1M test, but as discussed in Section 3.2.3, the

Semiscale heater rods experienced two temperature excursions during Test S-IB-3. The first excursion was due to a severe level depression in the vessel caused by the intact loop liquid seal; the second was due to a loss of steam cooling caused by the boiloff of core coolant to an elevation below the bottom of the heated length.^b Differences in pump suction elevations for the two facilities caused the extent of vessel level depression due to pump suction liquid seals to differ. In addition, the thermal responses were affected by differences in the elevations of the top and bottom of the core heated lengths and differences in the scaled downcomer volumes for the two facilities. The net result was that although the level depression in the vessel during Test B-R1M was almost as severe as that during Test S-IB-3 (see Figure 24), approximately one-fourth of the LOBI core^b remained covered, whereas the entire Semiscale core^b was uncovered. Also, during the period of boiloff of core coolant following the vessel level recovery, at least one-third of the LOBI core remained covered, whereas almost the entire length of the Semiscale core was uncovered.

a. The Test S-IB-3 break mass flow rate was calculated using the broken loop cold leg mass flows on each side of the break. The Test B-R1M break mass flow rate was calculated using the broken loop cold leg mass flows on each side of the break as given in Reference 3, where the reported mass flows have been divided by the volume scaling factor of 3.617.

b. As indicated by the collapsed liquid level; the swollen liquid level will be somewhat higher.

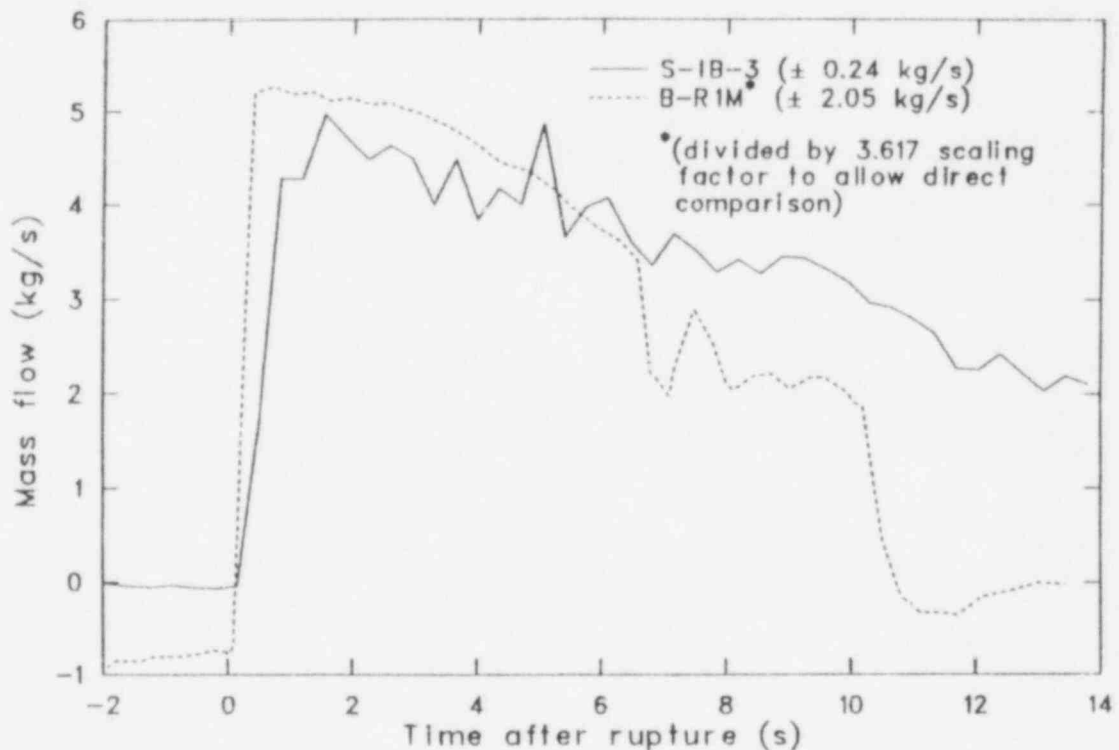


Figure 29. Comparison of break mass flow rates during Semiscale Test S-IB-3 and LOBI Test B-R1M.

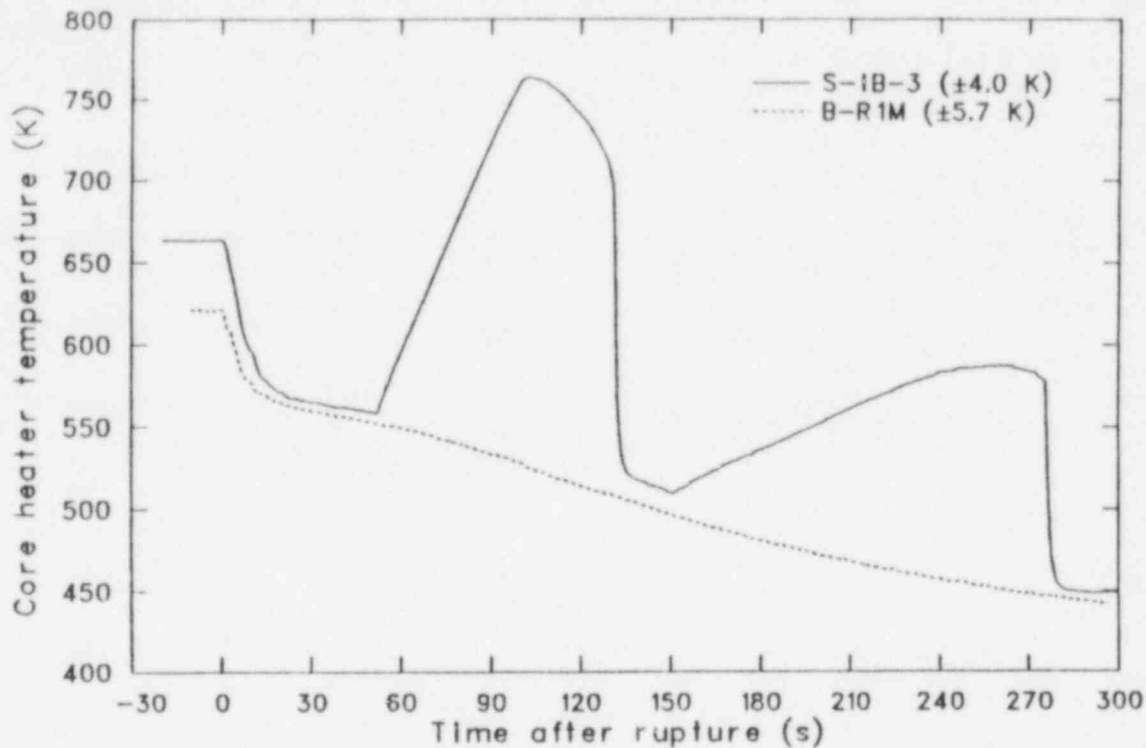


Figure 30. Comparison of peak heater rod temperature during Semiscale Test S-IB-3 and heater rod temperature at same relative elevation during LOBI Test B-R1M.

The minimal level boiloff after loop seal clearing during the LOBI test is a consequence of the LOBI facility having a larger than scaled downcomer volume. The larger downcomer liquid volume supplied more coolant to the LOBI vessel than was supplied to the Semiscale vessel. Thus, the vessel level during Test B-R1M was sufficient to allow low quality steam generation and maintenance of saturation temperatures in the core. However, the vessel level during Test S-IB-3 was not sufficient to allow low quality steam generation during parts of the test and saturation temperatures were not maintained in the core during the periods of insufficient steam generation. Therefore, although the core thermal responses during the two tests were not in good agreement, the causes of the discrepancies were configurational differences rather than phenomenological differences. A detailed discussion of the effects of scaled downcomer volume differences, as well as the effects of pump suction and core heated length elevation differences is contained in Section 3.4.2.

Discrepancies observed in the primary-to-secondary heat transfer during the two tests were due, in part, to differences in test conduct and initial conditions. Figure 31 shows that the LOBI intact and broken loop steam generators lost their

heat sink capabilities at about 35 s during Test B-R1M. The figure also shows that the Semiscale broken loop steam generator lost its heat sink potential at about 20 s, whereas the intact loop steam generator lost its heat sink potential between about 90 and 105 s during Test S-IB-3. The intact loop steam generator steam valve was not closed until the primary system pressure reached 1 MPa during Test S-IB-3, whereas the broken loop steam generator steam valve was closed at blowdown. The intact and broken loop steam generator steam lines were isolated very soon after blowdown during Test B-R1M. Also, the differences in initial conditions, shown in Table 4, contributed to the different secondary pressures observed in Figure 31. Transient secondary heat removal was therefore dissimilar between the two tests. The effects of the dissimilarity in secondary heat removal on the hydraulic responses during the two tests are discussed in Section 3.4.3.

In summary, the hydraulic responses during the two tests were very similar, but the thermal responses were quite different. The causes for the disparities were differences in system configuration and test conduct and are not believed to be indicative of phenomenological differences. Thus,

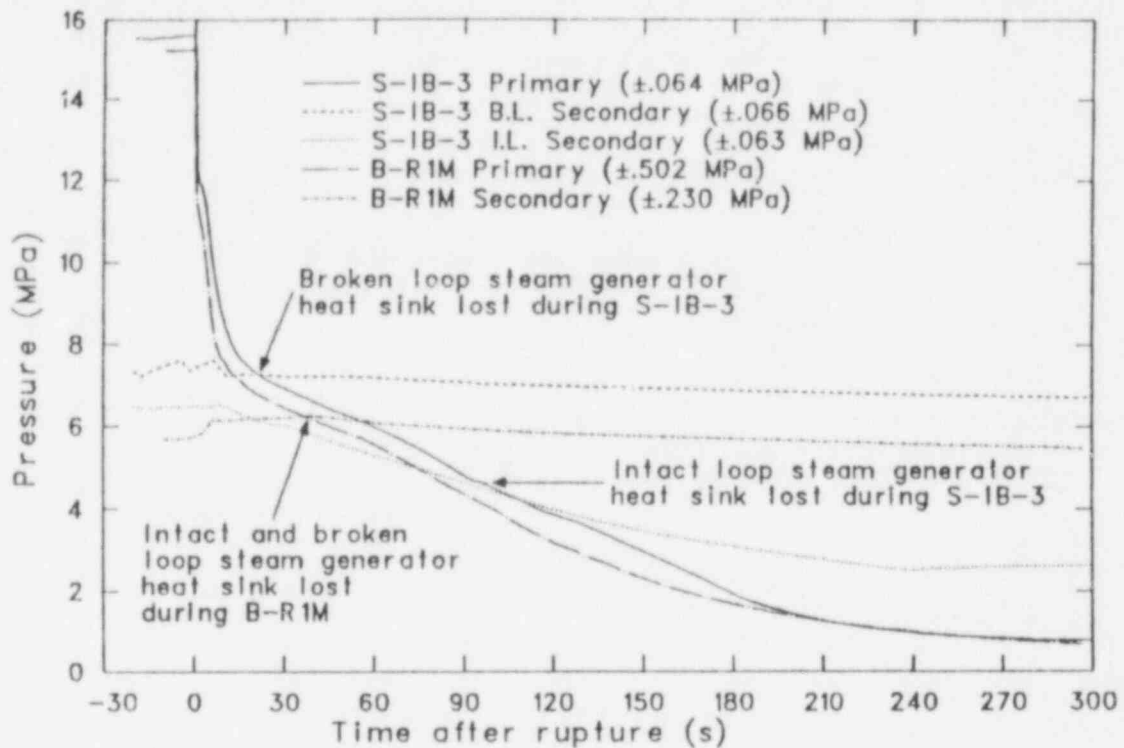


Figure 31. Comparison of primary and secondary pressures during Semiscale Test S-IB-3 and LOBI Test B-R1M.

the results obtained in the LOBI facility were essentially consistent with those obtained in the Semiscale Mod-2A facility.

3.4.2 Effects of Facility Configuration Differences. As already indicated, a number of configurational differences exist between the LOBI and Semiscale Mod-2A facilities. Consideration of the effects of these differences is instrumental in explaining some of the behavioral differences noted earlier. The following subsections present discussions of the effects on the test results of differences in (a) heater rod configuration, (b) downcomer configuration, and (c) pump suction and active core elevation. A comparison of the key parameters discussed and the counterpart parameters for a full-scale plant is contained in Table 5.

3.4.2.1 Effect of Heater Rod Configuration Differences—The LOBI heater rods are of a hollow tube design, which gives them less heat storage capacity than the solid rods in the Semiscale core. The power decay curve used during the LOBI B-R1M test was calculated to provide sufficient power to the heater rods to simulate the stored energy expected in the LOBI reference PWR nuclear fuel rods during a transient involving a

break size representative of 25% of the cold leg area of the reference PWR. Thus, the Test B-R1M power decay curve supplied the LOBI rods with the power necessary to make up for their low heat storage capacity. Due to the unavailability of detailed design information on the LOBI rods prior to the test, the B-R1M core power decay curve was used directly for the Semiscale counterpart test. This caused more power to be supplied to the Semiscale rods than was necessary to simulate the storage capacity of the LOBI reference PWR nuclear fuel rods. Also, the LOBI heater rods have a "flatter" axial power profile than the Semiscale heater rods, which causes the core power density for the two facilities to be different.

In an attempt to determine the quantitative effects of the differences in heater rod configurations, sensitivity calculations were performed with the RELAP5 computer code^{a,17} to determine how the Semiscale experiment might have behaved had LOBI heater rods been used. The results of these calculations are discussed in Appendix A.

a. RELAP5/MOD1, Cycle 18, is retained under INEL Computer Code Configuration Management (CCCM) Archival Number F00885.

Table 5. Comparisons of several key configuration parameters for Semiscale, LOBI, and a reference PWR

Configuration	Semiscale	LOBI	Reference PWR
Rod	Direct electrical heating of wound wire embedded in cylindrical rods	Direct electrical heating of walls of hollow tubes	Nuclear fuel rods
Downcomer volume percentage of total system volume	10.66	37.15	9.75 ^a
Pump suction and core [elevations relative to cold leg nozzle centerline (cm)]			
Intact loop pump suction	-282	-248 ^b	-314 ^a
Broken loop pump suction	-280	-203 ^b	-314 ^a
Top of core	-130	-201	-159 ^a
Bottom of core	-496	-591	-520 ^a

a. Values for reference PWR taken from Reference 2.

b. Approximate values.

Briefly, the calculations indicated that the different initial stored energy did not significantly affect the results, since it was dissipated within the first 25 s of the transient. The predicted effect of the differences in heater rod configurations and axial power profiles would be to cause the temperature excursion on the LOBI heater rod (in Semiscale) to be slightly less severe than the temperature excursion on the Semiscale heater rod (see Appendix A, Figure A-1). Thus, the predicted heater rod responses are very similar for the two configurations.

In summary, the effects of differences in heater rod configurations and axial power profiles on the test results probably caused a slight increase in the rate and magnitude of the temperature excursions during Test S-IB-3. The general trends observed in the thermal-hydraulic responses were otherwise unaltered.

3.4.2.2 Effect of Downcomer Configuration Differences—The annular LOBI downcomer utilized a

wider than scaled gap during the B-RIM test (50 mm versus 7 mm), which resulted in a low resistance to axial flow through the downcomer. The intact and broken loop hot legs are at essentially the same elevations as the cold legs. The resulting geometry creates a resistance to flow around the annulus from the intact loop cold leg to the broken loop cold leg. The Semiscale downcomer has an annular design at the inlet, but the majority of the downcomer is a single pipe. This inlet annulus design does not incorporate any restriction to flow around the annulus from the intact loop cold leg to the broken loop cold leg such as that created by the hot legs in the LOBI design. Also, the single-pipe downcomer in the Semiscale design prevents countercurrent flow to the extent that the LOBI annular downcomer design allows. Perhaps the most substantial cause of differences in the test results was the wider than scaled gap in the LOBI annular downcomer during the B-RIM test, which resulted in a larger than scaled volume in the downcomer (see Table 5). This caused the percentage of the primary coolant

system volume located in the reactor vessel to be substantially larger during the LOBI B-R1M test than during the Semiscale S-IB-3 test (57.7% versus 32.1%). Hence, for proportionately equal mass depletions, the liquid level in the Semiscale downcomer will decrease faster than in the LOBI downcomer.

The effects of the large LOBI downcomer gap and the associated oversized downcomer volume on the system behavior during large break tests performed in the LOBI facility are described in Reference 18. Briefly, the large downcomer volume results in more fluid remaining in the pressure vessel and in positive core mass flows during the late blowdown and refill period. This provides good cooling of the heater rod bundle during the entire transient. Also, the large downcomer gap results in better ECC penetration and a more typical refill of the pressure vessel than in Semiscale. Although these effects were determined from the results of large break tests, they are very similar for small break tests. The large downcomer volume will result in more fluid remaining in the pressure vessel than for the scaled downcomer volume, regardless of the break size. The larger downcomer volume also supplies more coolant to the core following loop seal clearing.

Hence, more coolant, and consequently better cooling, is provided to the heater rod bundle during the transient.

The effect of the single-pipe design and the lack of a restriction to flow around the inlet annulus in the Semiscale downcomer is to inhibit ECC penetration and refilling of the pressure vessel.

Thus, one effect of the larger LOBI downcomer volume was to supply more coolant to, and better cooling of, the heater rods during Test B-R1M than that which occurred during Test S-IB-3. Another effect of the differences in downcomer design was to cause more bypass of ECC fluid from the intact to the broken loop cold leg during the Semiscale test than occurred during the LOBI test. As shown in Figure 32, the initiation of accumulator injection occurred at approximately 139 s during Test B-R1M and at approximately 163 s during Test S-IB-3. However, as shown in Figure 24, the refilling of the pressure vessel started at about 150 s during Test B-R1M and at about 190 s during Test S-IB-3. The smaller delay between initiation of accumulator injection and the start of pressure vessel refilling during Test B-R1M (11 s versus 27 s) is attributed to better ECC penetration afforded by the large downcomer gap.

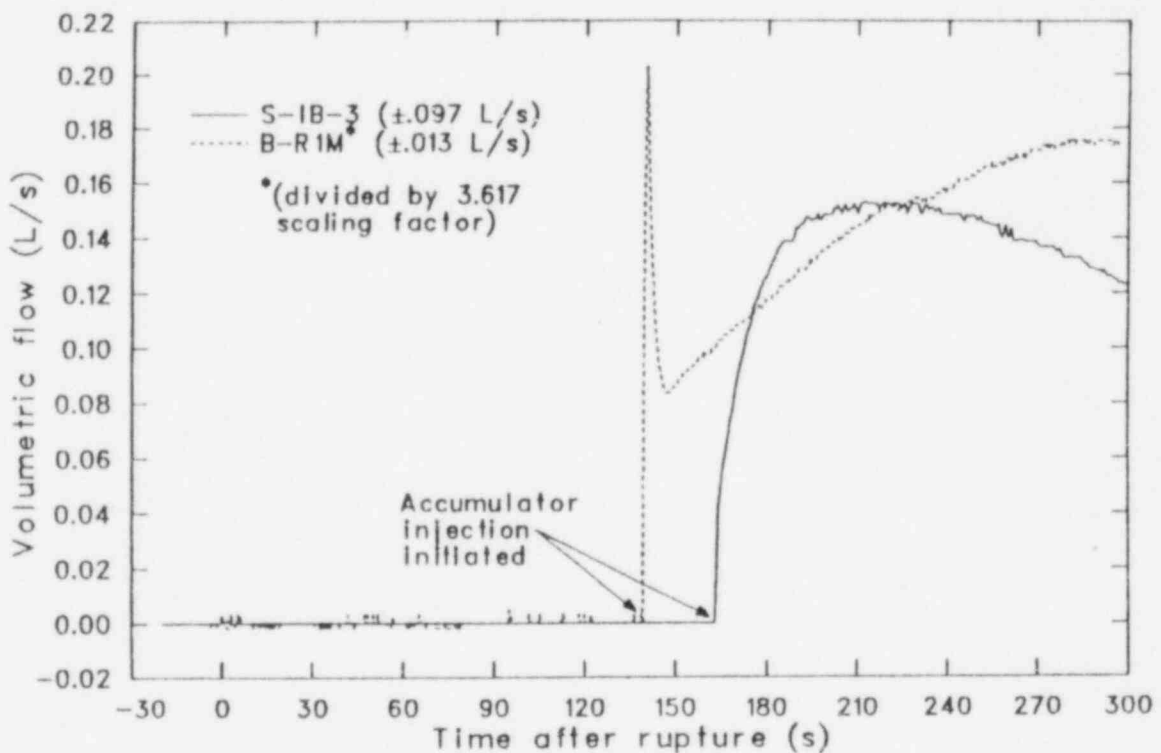


Figure 32. Comparison of accumulator volumetric flow rates during Semiscale Test S-IB-3 and LOBI Test B-R1M.

In summary, the effect of the differences in downcomer configurations was to afford better cooling in the core during Test B-R1M than occurred during Test S-IB-3. Thus, the differences in downcomer configurations were instrumental in causing the differences in core thermal response noted in Section 3.4.1.

3.4.2.3 Effect of Pump Suction and Core Elevation Differences—The bottom of the loop pump suctions are farther below the cold leg centerline elevations in Semiscale than they are in LOBI. Furthermore, the top and bottom of the core heated lengths are farther below the cold leg centerline elevations in LOBI than they are in Semiscale. Table 5 shows the magnitude of the differences in pump suction and core elevations for the two facilities.

The differences in pump suction elevations causes the vessel level depression, due to pump suction seal formation, to be less severe in the LOBI facility than in the Semiscale facility. This is because a smaller pressure differential across the pump suctions is required to overcome the liquid gravity head in the LOBI pump suctions than that in the deeper Semiscale pump suctions. As shown in Figure 24, the level depression in the vessel during loop seal formation was more severe during the Semiscale test than during the LOBI test.

Because the LOBI core is longer and the top of it is lower than the Semiscale core, the bottom is almost 100 cm deeper in the vessel than is the bottom of the Semiscale core heated length. This deeper core positioning allows the LOBI heater rods to remain partially covered with proportionately smaller amounts of coolant. As shown in Figure 24, the bottom 100 cm of the LOBI core remained covered during the period of depressed vessel level.

In summary, the effects of the pump suction and core elevation differences on the test results are additive; the net effect is that the LOBI core remained at least partially covered^a during the transient, whereas the Semiscale core was completely uncovered^a during parts of the transient. The steam generated from the covered portion of the LOBI core is believed to have been sufficient to maintain saturated conditions in the core throughout the B-R1M transient. In contrast, the complete uncovering of the Semiscale core is

a. As indicated by collapsed liquid level; the swollen liquid level will be somewhat higher.

believed to have caused a lack of sufficient steam generation to maintain saturation conditions in the core during parts of the S-IB-3 transient. Hence, the differences in elevations were also instrumental in causing the differences in core thermal responses noted in Section 3.4.1.

3.4.3 Effects of Differences in Test Conduct. Several minor differences in test conduct existed between Tests S-IB-3 and B-R1M, but are believed to have had no significant effect on the test results. However, a major difference in steam generator operation did have some effect on the results. As indicated earlier, both steam generators were isolated at blowdown during Test B-R1M. During Test S-IB-3, however, the broken loop steam generator was isolated at blowdown, but the intact loop steam generator steam line was not isolated until the primary system pressure reached 1 MPa. The possible effects of this asymmetric operation of the steam generators on the Test S-IB-3 results are discussed in Reference 8. Briefly, it is postulated that the early isolation of the broken loop steam generator in Semiscale caused early clearing of the broken loop pump suction, which in turn caused a delayed clearing of the intact loop pump suction.

In an attempt to determine the effects of the differences in steam generator operation, sensitivity calculations were performed using the RELAP5 computer code, first with both steam generator steam lines isolated at blowdown, and then with both steam lines remaining unisolated until the primary system pressure reached 1 MPa. The results of these calculations are discussed in Appendix A.

Briefly, the isolation of both steam generators at blowdown caused an earlier loss of the intact loop steam generator secondary heat sink, which affected the transient in two ways. One effect was to cause a higher primary system pressure, which resulted in a higher break flow rate. Consequently, more primary system mass was lost during the first 75 s of the transient. The second effect was to cause a reduced potential for condensation in the intact loop steam generator U-tubes. After the primary system pressure dropped below the intact loop steam generator pressure, the potential for condensation was lost and the intact loop seal was allowed to clear. The intact loop pump suction upflow side cleared earlier for the symmetric steam generator isolation case than it did for the calculation that was performed using asymmetric operation of the steam generators, similar to

that which occurred during Test S-IB-3 (see Appendix A, Figure A-2). As expected, the earlier clearing of the intact loop seal is calculated to cause earlier vessel level recovery (see Appendix A, Figure A-3). In addition, the earlier clearing of the intact loop seal for the symmetric steam generator isolation case allowed the vessel level to recover while more mass was in the downcomer. Hence, the vessel level recovered to a higher level and the boiloff of core coolant after loop seal clearing was more prominent than in the reference case.

Delaying the isolation of the steam lines for both steam generators is calculated to have no effect on the calculated transient response. The clearing time of the broken loop pump suction upflow leg was almost identical to that for the case of asymmetric steam generator operation. In addition, the vessel level depression was almost identical for both calculations (see Appendix A,

Figures A-4 and A-5). This lack of sensitivity to broken loop steam generator secondary conditions indicates that the 21.7% break size is large enough to control broken loop seal clearing.

In summary, the results of the sensitivity calculations indicate that late isolation of the intact loop steam generator steam line caused delayed clearing of the intact loop seal, and that the operation of the broken loop steam generator steam line had essentially no effect on the transient. Thus, the operation of the broken loop steam generator probably did not cause the delayed clearing of the intact loop seal as previously reported.⁸ Rather, the operation of the intact loop steam generator during Test S-IB-3 contributed to the differences observed in the intact loop seal clearings and vessel level depressions in the two facilities (discussed in Section 3.4.1).

4. CONCLUSIONS

Analyses of the results of the Semiscale Mod-2A Intermediate Break Test Series led to the following conclusions:

1. Comparisons of the thermal and hydraulic responses during Semiscale intermediate, large, and small break tests resulted in the characterization of the phenomena observed to be important during each of the intermediate break tests. Large break hydraulic behavior appears to persist down to break sizes of 50%. Somewhere between 50 and 21.7%, gravity dominance begins to override and small break behavior prevails. These results therefore suggest a threshold break range, either side of which the modeling of full-scale plant loss-of-coolant accidents should seek to describe different thermal and hydrodynamic behavior. Inertially dominated flows, ECC bypass, and post-critical-heat-flux and reflood heat transfer are important during large breaks. Conversely, gravity-dominated flows, pump seal behavior, slow core uncover heat transfer, elevation effects, and steam generator heat transfer become important during small breaks.
2. The limited results from the intermediate break tests in Semiscale have not uncovered any thermal-hydraulic phenomena not already evidenced in either large or small break tests previously conducted.
3. Comparisons of results from the Semiscale 21.7% break test with LOBI and LOFT test results indicate very similar behavior despite the span in scale size from 1/1700 to 1/60. This augments the already existing evidence that the basic scaling criteria underlying these facilities are sound. However, an orderly examination of the behavioral differences that did occur between the systems highlights the significant roles that certain configurational aspects have in determining small break results. Specifically, primary coolant volume distribution, component elevation relationships, and steam generator operation can substantially influence the severity of small break loss-of-coolant transients. Consequently, preserving these relationships between scale model and prototype will enhance scaled model test results.

5. REFERENCES

1. *System Design Description for the Mod-3 Semiscale System*, Addendum 1, "Mod-2A Phase 1 Addendum to Mod-3 System Design Description," December 1980.
2. T. K. Larson, J. L. Anderson, D. J. Shimeck, *Scaling Criteria and an Assessment of Semiscale Mod-3 Scaling for Small Break Loss-of-Coolant Transients*, EGG-SEMI-5121, March 1980.
3. C. Addabbo, G. DeSanti, L. Piplies, *Quick Look Report on LOBI Test B-R1M*, LQC 82-08, March 1982.
4. A. G. Stephens, *Experiment Operating Specification for Semiscale Mod-2A Experiments S-IB-1 and S-IB-2*, EGG-SEMI-5722, January 1982.
5. T. J. Boucher, *Experiment Operating Specification for Semiscale Mod-2A Experiment S-IB-3*, EGG-SEMI-5787, February 1982.
6. A. G. Stephens and C. M. Kullberg, *Quick Look Report for Semiscale Intermediate Break Test S-IB-1*, EGG-SEMI-5859, April 1982.
7. A. G. Stephens, C. M. Kullberg, T. J. Boucher, *Quick Look Report for Semiscale Intermediate Break Test S-IB-2*, EGG-SEMI-6021, August 1982.
8. T. J. Boucher and M. T. Leonard, *Quick Look Report for Semiscale Intermediate Break Test S-IB-3*, EGG-SEMI-6013, August 1982.
9. R. G. Hanson, *Quick Look Report for Semiscale Mod-3 Tests S-07-8 and S-07-9 Baseline Test Series*, SEMI-TR-007, May 1979.
10. J. E. Blakely, R. G. Hanson, D. J. Shimeck, *Quick Look Report for Semiscale Mod-2A Test S-UT-1*, EGG-SEMI-5331, January 1981.
11. M. T. Leonard, *Vessel Coolant Mass Depletion During A Small Break LOCA*, EGG-SEMI-6010, September 1982.
12. D. B. Jarrell and J. M. Devine, *Experiment Data Report for LOFT Intermediate Break Experiment L5-1 and Severe Core Transient Experiment L8-2*, NUREG/CR-2398, EGG-2136, November 1981.
13. J. P. Adams, *Quick Look Report on LOFT Nuclear Experiments L5-1 and L8-2*, EGG-LOFT-5625, October 1981.
14. V. T. Berta, private communication, LOFT Program, EG&G Idaho, Inc., January 17, 1983.
15. L. Piplies, *Thermohydraulic Specifications of the Ispra Blowdown Loop*, Technical Note I.06.00.77.75, J.R.C. Ispra, November 1977.
16. E. Ohlmer and J. Sanders, *Experimental Data Report on LOBI Test B-R1M*, LEC 82-08, April 1982.
17. V. H. Ransom et al., *RELAP5/MOD1 Code Manual*, NUREG/CR-1826, EGG-2070, March 1982.
18. H. Stadtke, D. Carey, W. L. Riebold, "Influence of Downcomer Volume and Gap Width on Blowdown," *International Meeting on Thermal Nuclear Safety, Chicago, Illinois, August 29-September 2, 1982*.

APPENDIX A
RELAP5 SENSITIVITY STUDIES

APPENDIX A

RELAP5 SENSITIVITY STUDIES

Sensitivity calculations were performed to determine the effect of (a) heater rod geometry, and (b) steam generator operating conditions on Test S-IB-3 results as they related to the LOBI B-RIM test. The calculations were performed with the RELAP5/MOD1 (Cycle 18) computer code^{A-1} and employed the standard Semiscale model as documented in Reference A-2. Initial conditions in the computer analyses were similar to those of Test S-IB-3 and resulted in analytical results qualitatively similar to the test. The following operating conditions were observed in the test and were used in the RELAP5 analyses.

1. Steam generator: (a) feedwater to both steam generators isolated at break initiation, (b) broken loop steam generator steam valve closed at break initiation, and (c) intact loop steam generator steam valve open until low pressure injection system (LPIS) actuation.
2. LPIS: actuation at 1.0 MPa pressurizer pressure.
3. Guard heaters turned off for entire test, but system heat losses modeled.
4. Primary coolant pumps: both pumps operated as described in the S-IB-3 Quick Look Report (QLR).^{A-3}
5. Core power history: core power as reported in the S-IB-3 QLR.
6. Accumulator: accumulator setpoint as described in the S-IB-3 Experiment Operating Specification (EOS).^{A-4}

Four RELAP5 calculations were performed for the sensitivity study.

1. A reference case was completed in which steam generator operations and fuel rod geometry were the same as during Test S-IB-3.
2. A heater rod geometry sensitivity case was generated by replacing the Semiscale heater rod geometry with that characteristic of the

LOBI^{A-5} facility. Using the same power input as Test S-IB-3 resulted in a lower initial stored energy for the LOBI configuration.

3. Two cases using symmetrical steam generator operating conditions were calculated. In the first, both steam generators were isolated at the time of break initiation; in the second, both steam valves were maintained at their initial position until the time of LPIS actuation. In both of these symmetrical operating cases, all other system parameters were the same as the reference case.

Heater Rod Geometry Sensitivity

The sensitivity of the transient response to heater rod geometry was investigated by replacing the Semiscale heater rod model with one representative of a LOBI heater rod. Although the LOBI heater rods are longer and more massive than Semiscale rods, their hollow construction and lower axial power peaking factor^{A-5} resulted in lower initial stored energy than in Semiscale. The RELAP5 calculation using the LOBI heater rod geometry gave hydraulic results similar to the reference case, including blowdown rates, system depressurization rates, loop seal clearing times, and core liquid level depression. As shown in Figure A-1, both calculations demonstrated a heater rod surface temperature excursion beginning at about 65 s after break initiation. The heatup was caused by the loss of surface cooling resulting from the core level depression, and was independent of the initial stored energy, which was dissipated within the first 25 s of the transient. The temperature rise was driven by the local power density and occurred even with a linear heat generation rate characteristic of the LOBI 64-rod core.

The conclusion of the sensitivity study was that the Semiscale heater rod geometry and axial power profile would not cause a heater rod response significantly different from that of a LOBI heater rod.

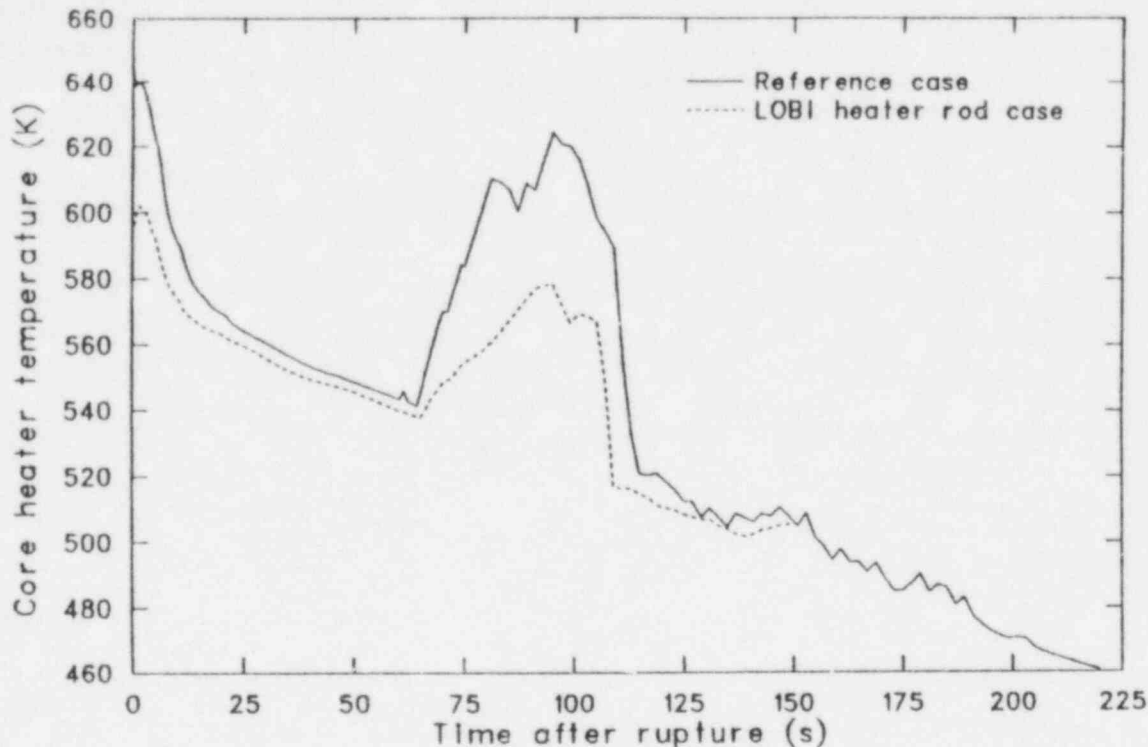


Figure A-1. Comparison of calculated heater rod temperatures for reference case and for LOBI heater rod case.

Steam Generator Operating Conditions Sensitivity

The effect of asymmetric steam generator operation in Test S-IB-3 was determined by running two sensitivity calculations, one in which both the intact and broken loop steam generators were isolated on break initiation (symmetric isolated case), and one in which both the intact and broken loop steam generators were left steaming until LPIS initiation (symmetric steaming case). The effects of steam generator operation were evaluated in terms of loop seal clearing time (as measured by differential pressure in the pump suction leg) and core liquid level depression.

The difference from the reference case introduced by symmetric isolated operation was removal of the intact loop steam generator secondary heat sink by closing the steam valve on break initiation. This precluded a rapid depressurization of the intact loop steam generator and resulted in primary system pressure staying higher than the reference case. This caused two noticeable differences in the transient. First, the higher system pressure resulted in a higher primary break flow rate; approximately 10% more primary system mass

was lost during the first 75 s of the transient. Second, the higher secondary side pressure resulted in a reduced condensation potential in the intact loop steam generator U-tubes. The reduced condensation potential allowed both the intact loop hot leg and the downcomer to reverse flow early in the transient, whereas the reference case maintained forward (normal direction) flow in both locations. Intact loop pump suction coolant level maintained a loop seal until shortly after the primary system pressure dropped below the intact loop steam generator pressure, thus removing the condensation potential and allowing the loop seal to clear. Figure A-2 shows the intact loop pump suction level on the upside clearing between 60 and 80 s for the symmetric isolated calculation. The steam generator steaming condition maintains the condensation potential until about 140 s. Figure A-2 shows the reference case intact loop pump suction clearing at about this same time. The earlier clearing of the pump suction loop seal in the symmetric isolated case allows an earlier recovery of the core collapsed liquid level, as shown in Figure A-3.

The symmetric steaming case differed from the reference case in that the broken loop steam

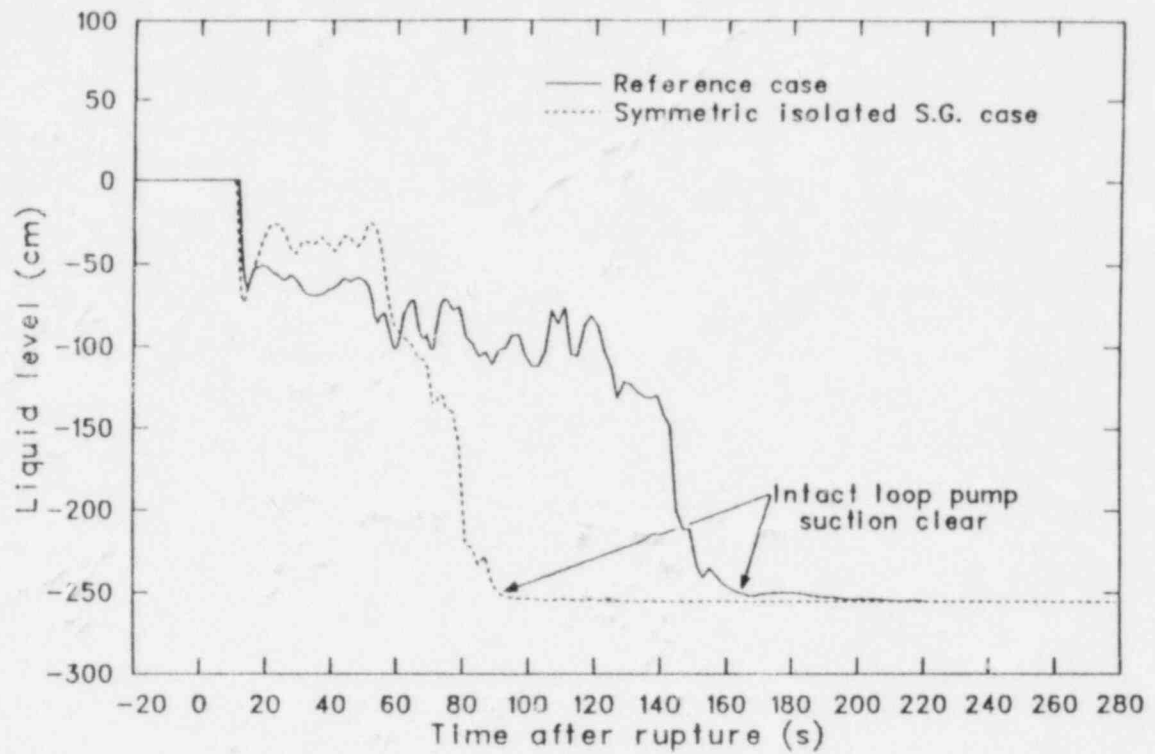


Figure A-2. Comparison of intact loop pump suction upflow side liquid levels calculated for reference case and for the symmetric isolated steam generator operation case.

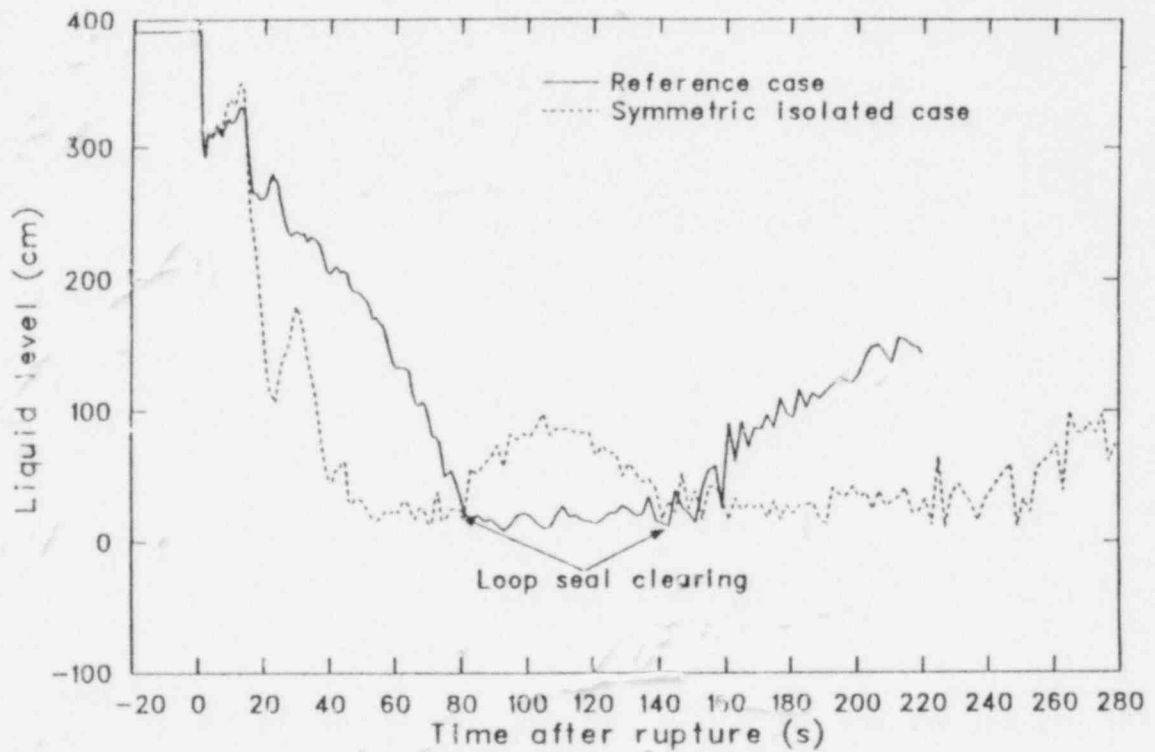


Figure A-3. Comparison of vessel collapsed liquid levels calculated for the reference case and for the symmetric isolated steam generator operation case.

generator continued steaming until LPIS initiation. The results of this calculation were almost identical to the reference case, as seen in Figures A-4 and A-5. Broken loop seal clearing times and core collapsed liquid levels showed essentially no sensitivity to broken loop steam generator operating conditions during Test S-IB-3. This indicated that the break size was sufficiently large to dominate broken loop seal clearing, independent of the effect of condensation in the broken loop steam generator.

In summary, for the conditions of Test S-IB-3, intact loop steam generator operating conditions are seen to significantly impact transient behavior by affecting the major system heat sink. Removal of the heat sink (by closing the steam valve) resulted in a more rapid primary system mass loss due to higher primary coolant system pressure and a quicker clearing of the intact loop pump suction loop seal. Broken loop steam generator secondary conditions were seen to have a minimal impact on the transient results.

References

- A-1. V. H. Ransom et al., *RELAP5/MOD1 Code Manual*, NUREG/CR-1826, EGG-2070, March 1982.
- A-2. M. T. Leonard, *RELAP5 Standard Model Description for the Semiscale Mod-2A System*, EGG-SEMI-5692, December 1981.
- A-3. T. J. Boucher and M. T. Leonard, *Quick Look Report for Semiscale Intermediate Break Test S-IB-3*, EGG-SEMI-6013, August 1982.
- A-4. T. J. Boucher, *Experiment Operating Specification (EOS) for Semiscale Mod-2A Experiment S-IB-3*, EGG-SEMI-5787, February 1982.
- A-5. W. Riebold et al., *Specifications, LOBI Pre-Prediction Exercise, Influence of PWR Primary Loops on Blowdown (LOBI)*, Technical Note Nr. 1.06.01.79.25, February 1979.

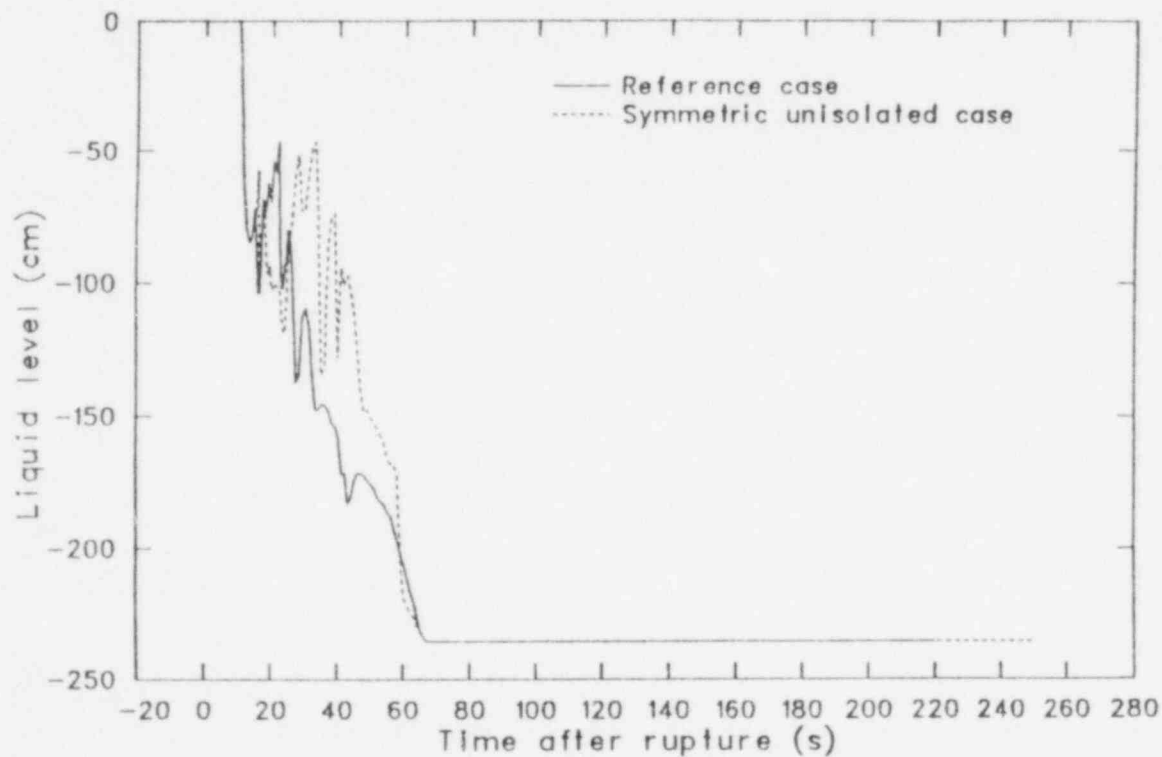


Figure A-4. Comparison of intact loop pump suction upflow side liquid levels calculated for the reference case and for the symmetric unisolated steam generator operation case.

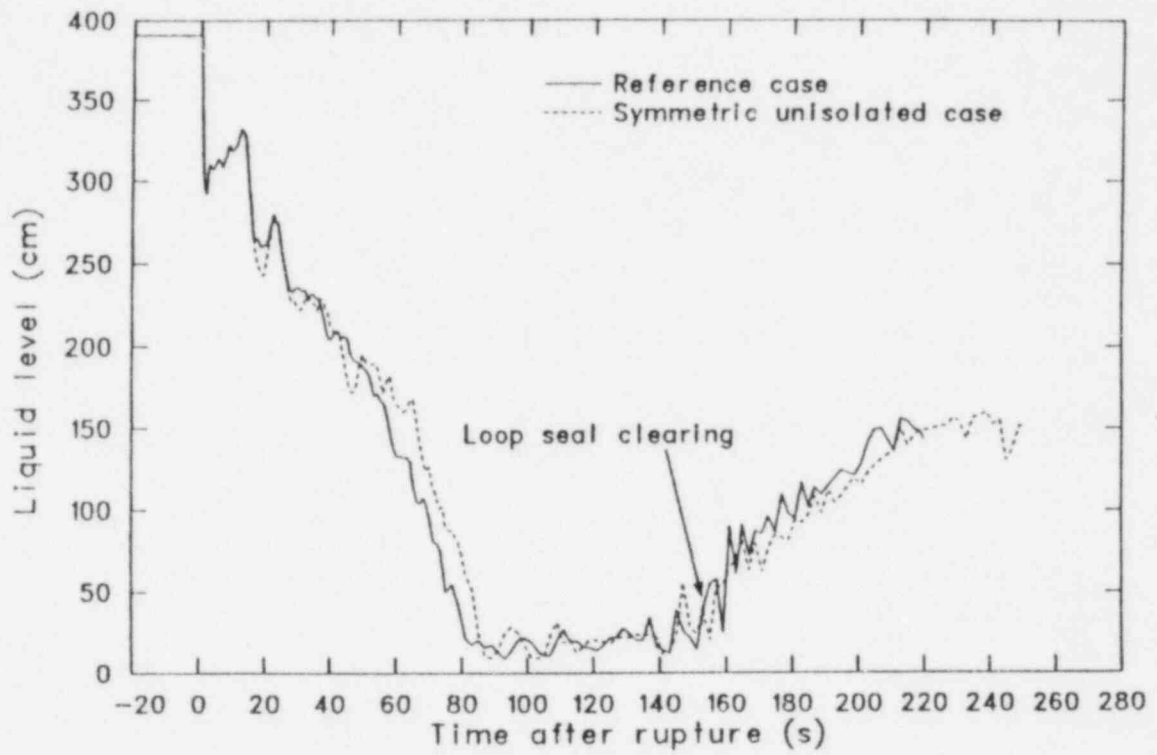


Figure A-5. Comparison of vessel collapsed liquid levels calculated for the reference case and for the symmetric unisolated steam generator operation case.